1960

Investigation of the free convection heat transfer characteristics of single horizontal screen matrices.

Metschel, John J.

Monterey, California: U.S. Naval Postgraduate School

INVESTIGATION OF THE FREE CONVECTION HEAT TRANSFER CHARACTERISTICS OF SINGLE HORIZONTAL SCREEN MATRICES

JOHN J. METSCHEL

INVESTIGATION OF THE FREE CONVECTION HEAT TRANSFER CHARACTERISTICS OF SINGLE HORIZONTAL SCREEN MATRICES

****

John J. Metschel

INVESTIGATION OF THE FREE CONVECTION HEAT TRANSFER CHARACTERISTICS OF SINGLE HORIZONTAL SCREEN MATRICES

by

John J. Metschel

This work is accepted as fulfilling
the thesis requirements for the degree of
MASTER OF SCIENCE
IN
MECHANICAL ENGINEERING
from the
United States Naval Postgraduate School

INVESTIGATION OF THE FREE CONVECTION HEAT TRANSFER CHARACTERISTICS OF SINGLE HORIZONTAL SCREEN MATRICES

by

John J. Metschel
Lieutenant Commander, United States Navy

Submitted in partial fulfillment of
the requirements for the degree of
MASTER OF SCIENCE
IN
MECHANICAL ENGINEERING

United States Naval Postgraduate School
Monterey, California
1960

ABSTRACT

Free convection heat transfer characteristics were determined for single, horizontal, woven-wire screen matrices with meshes varying from a 10 x 10 to a 60 x 60 mesh.

A transient technique employing radiant heating was developed to obtain data.

Experiments were performed in still air at normal room temperatures with matrix temperatures as high as 137 degrees Fahrenheit above room temperature for the 60 x 60 mesh, and 55 degrees Fahrenheit above room temperature for the 10 x 10 mesh.

The heat transfer characteristics of the screen matrices were determined using (1) the screen wire diameter as the characteristic dimension, and (2) the overall screen size as the characteristic dimension. This is presented in the form of a Nusselt number as a function of the product of the Grashof and Prandtl numbers correlation.

Free convection heat transfer characteristics were also obtained for solid plates of the same size as the screen matrices. These data were used to provide: (1) an indication of the accuracy of results obtained by the experimental technique and instrumentation, and (2) a comparative reference as a zero porosity matrix.

ACKNOWLEDGEMENTS

The author wishes to thank P. Pucci, Associate Professor of Mechanical Engineering, for his guidance and under whose direction this work was carried out. My thanks also to C. Howard, Assistant Professor of Mechanical Engineering, for his aid and suggestions on various problems encountered in this project.

Grateful acknowledgements are also extended to my father-in-law, Lt. Col. R. O. Hillis, for manufacturing the patterns and jig for the reflector, and to my wife, Judy, for her assistance in write-ups and calculations.

TABLE OF CONTENTS

LIST OF ILLUSTRATIONS

LIST OF TABLES

LIST OF SYMBOLS AND ABBREVIATIONS

English Letter Symbols

A	Total heat transfer area, ft^2
C	Generalized constant
c_p	Specific heat at constant pressure, BTU/lbm °F
d	Diameter of screen wires, ft
D	Plate or screen diameter, ft
g	Acceleration due to gravity, $g = 32.2$ ft/sec^2
h	Combined heat transfer coefficient, BTU/hr ft^2°F
h_c	Heat transfer coefficient for thermal free convection, BTU/hr ft^2°F
h_r	Heat transfer coefficient for thermal radiation, BTU/hr ft^2°F
k	Unit thermal conductivity, BTU/(hr ft^2°F/ft)
ℓ	Length, ft
m	Mass, lbm
q	Heat transfer rate, BTU/hr
t	Temperature, °F
t_a	Ambient temperature, °F
t_o	Temperature at time zero, °F
T_a	Absolute temperature of the ambient, °R
T_o	Absolute temperature at time zero, °R

Greek Letter Symbols

β	Coefficient of thermal expansion, 1/°R
ρ	Density, lbm/ft^3
μ	Viscosity, lbm/hr ft

σ	Stefan-Boltzman constant, 1.714×10^{-9} BTU/hr $ft^2 \cdot R^4$
ϵ	Emissivity
θ	Time, seconds
ϕ	Function symbol

Dimensionless Groupings

Nu	Nusselt number	$\left(\frac{hl}{k}\right)$
Gr	Grashof number	$\left(\frac{g\beta^2\rho^2\Delta t l^3}{\mu^2}\right)$
Pr	Prandtl number	$\left(\frac{\mu C_p}{k}\right)$

Force and Mass Units

lb	Denotes pound force
lbm	Denotes pounds mass

1. Introduction

Porous media are defined as solid matrices possessing a high ratio of void surface area to bulk volume and a void geometry that permits flow of gas or liquid through the matrix. Examples of porous media are woven wire screens, sintered metals, granular or spherical packed beds, and certain underground formations.

Typical applications of porous media are packed screens for regenerative heat exchangers, checkered brickwork for regenerative heating in furnace, granular packing in stripping columns and catalyst beds, and cores for nuclear reactors. In the petroleum industry the forcing of oil and gas through underground formations is important.

A great amount of data pertaining to heat transfer in porous media has been gathered and correlated in the field of forced convection. An excellent discussion and review is given by J. E. Coppage [1][1]. Less work has been done with natural convection and most of that in relation to underground formations. A review of this work is described by Rodger and Morrison [2].

In all of the above investigations interest was centered either on the forced convection aspects in which numerous types of geometries were considered, or the free convection aspects where the geometries investigated were thick slabs of porous media in such forms as packed beds of gravel or subterranean deposits of sand.

In the present study, attention is centered on the free convection heat transfer properties of thin slabs of porous media under conditions of free and horizontal suspension in air. Typical examples of such thin

[1]Number in brackets refer to reference in the Bibliography.

slab media are: perforated sheet metal, thin sheets of sintered metal, expanded metal, and in particular, the woven wire screens used in this investigation.

To the author's knowledge, no previous study has been made of the free convection heat transfer characteristics of thin slab porous media. The probable reasons are that the information is not in pressing demand and that accurate information is difficult to obtain. However, in view of the fact that porous sheets of many geometries and materials are on the market, it is felt that a basic study should be made to probe their potential of application.

A possible application of thin sheet matrices might be found in the aircraft electronics industry. Miniaturization of parts, compacting of assemblies, reduction in weight specifications, and increased power levels have made heat removal a severe problem. Present designs for cooling consist of feeding low pressure air to sub assemblies or "black boxes". Each black box is an airtight envelope housing a chassis and its components. Control of the flow pattern through the maze of components in each black box is extremely difficult. Dead spots and areas of poor circulation are numerous and result in frequent component failures by overheating. It is possible that should selected chassis areas be made of porous sheeting, circulation might be improved and dead spots eliminated.

This present investigation is limited to porous sheet material in the form of stainless steel woven wire screens. The solid flat plate is used as a parameter for comparison.

2. Objective

The objective of this investigation was to develop a testing technique to determine the natural convection heat transfer data for solid flat plates and wire screen matrices under conditions of free and horizontal suspension.

Background for Investigation

The solid flat plate might be considered as a matrix with zero porosity. Along the same lines of thought, a single horizontal wire might be considered as a matrix of infinite porosity. By intuition it appears that perhaps a wire screen would have characteristics intermediate between the geometries mentioned. With this in mind, a brief summary of the free convection results for horizontal wires and horizontal flat plates is presented.

Nusselt (1915) seems to have first employed the principle of similarity in free convection, [10] when he stated the general equation: that:

$$Nu = \phi (Gr, Pr)$$

and the simpler form:

$$Nu = \phi (Gr \cdot Pr)$$

if the inertia terms in the Stokes formulas are negligible compared to the viscosity terms. A. H. Davis (1922) found that his experiments on thin platinum wires in several kinds of fluids could be represented by the second relationship [11]. Nusselt in 1929 generalized the results of his first correlations using the second equation. Today, the second form of the equation is used almost universally and represents the fundamental relationship to describe free convective heat transfer.

Numerous investigations have been made for horizontal cylinders and plane vertical surfaces, both in air and in liquids. Unfortunately, other shapes have not been studied extensively. Some data is available for vertical cylinders and for horizontal plates facing upwards and downwards in air. Otherwise, only scattered information is available.

Most of the significant results for single horizontal cylinders have

[3] and Jakob [4].

$$Nu = 0.53\,[Gr \cdot Pr]^{1/4} \quad ; \quad 10^3 < Gr\,Pr < 10^9$$

and per Jakob:

$$Nu = 0.52\,[Gr\,Pr]^{1/4} \quad ; \quad Gr\,Pr \geq 10^9$$

Fischenden and Saunders [5] investigated horizontal plates facing both upwards and downwards. The surfaces used were rectangular or square. For rectangular plates, the mean edge length was taken as the characteristic dimension. The largest size investigated was two feet square. The maximum temperature used was in excess of 1000°F. The equations relating their findings are:

(a) For heated plates facing upward or cooled plates facing downward:

$$Nu = 0.14\,[Gr\,Pr]^{1/3} \quad ; \quad 2\times10^7 < Gr\,Pr < 3\times10^{10}$$
$$Nu = 0.54\,[Gr\,Pr]^{1/4} \quad 10^5 < Gr\,Pr < 2\times10^7$$

(b) For heated plates facing downward or cooled plates facing upward:

$$Nu = 0.27\,[Gr\,Pr]^{1/4} \quad ; \quad 3\times10^5 < Gr\,Pr < 3\times10^{10}$$

Jakob and Linke [9] later conducted experiments using boiling water on the upper side of horizontal plates. They found:

$Nu = 0.273\,[Gr\,Pr]^{1/3}$ in the turbulent region.

They furthermore concluded that the heat transfer in the turbulent region is independent of location, except perhaps close to the edge.

In 1935, R. Weise [6] determined the temperature distribution of the air surrounding heated horizontal plates. He used square aluminum plates 16 and 24 centimeters in side length and 1.0 and 1.5 centimeters

thick respectively. The plates were heated electrically and suspended in a wide room. Weise calculated the local coefficients of heat transfer from the temperature gradients close to the plate to check the overall coefficient found by direct measurement. His results were in good agreement with previous investigators.

4. Experimental Method

Two broad techniques are available for determining free convection heat transfer coefficients: - the steady state method, and the transient method. The capabilities and limitations of each relevant to screen matricies are discussed below.

The principle advantage of the steady state method is the simplicity in calculating the heat transfer coefficients from experimental data. With respect to screen matrices, the chief disadvantage is in the difficulty in providing an internal source of heat that will produce a uniform temperature over the exterior surface of the test specimen. Scaled up models could be used. They would, however, have to be large in cross section to accomodate the heating elements and large in frontal area to offset edge effects. Several models would be necessary since the geometry of each of the screens is different. Fabrication of the models would be expensive. The probability of attaining uniform surface temperature for various conditions of flow would be doubtful. For these reasons, a steady state method was not used.

The transient method, although it has certain limitations, appeared to be suitable for this investigation.

Essentially, the transient technique consists of establishing an initial temperature difference between a body and its ambient fluid by heating or cooling and then recording the time temperature history of the body as it returns to equilibrium with the ambient [7].

Figure 15 shows a simple thermal circuit representing this system.

To use the technique effectively [7] the following conditions must be met:

(a) The thermal conductivity of the body is infinitely large.

(b) The body is at uniform temperature at time zero.

(c) Fluid flow equilibrium is established at time zero.

(d) The body must be treated as a single lumped thermal capacitance.

Condition (a) is approached practically by using bodies that have a large surface to volume ratio such as small wires and thin plates. According to Geidt [8] this condition is closely approximated if

$$\frac{k}{h\ell} \geq 2$$

Where k is the thermal conductivity of the body, h is the total heat transfer coefficient and ℓ is the smallest dimension.

To meet condition (b) two methods of heating are available:

Preheating the screens to uniform temperature before placing them in test position.

Using radiant heat and adjusting the incident radiation to produce uniform temperature with screens in test position.

Both methods are about equal in meeting condition (b).

The third condition (c) reduces the selection of a heating method to that of radiant heating. Preheating can be used in a free convection transient method if the mass of the object tested is large and its cooling rate is slow. This permits fluid flow to be established in the early part of the run. However, in this investigation the mass of the test specimen is relatively small and the cooling rate is fast. Therefore, it is necessary to establish fluid flow equilibrium before time zero. The radiant heating method only is capable of meeting this requirement. In addition, radiant heating provides for instantaneous and complete removal of heat source at time zero.

The fourth condition (d) specifies that the individual components of the total heat transfer coefficient cannot be separated by measurement. Thus, it is necessary to reduce parasitic heat losses such as heat conduction via thermocouple leads and heat transfer via supports to a negligible value. Heat transfer coefficients for convection and for radiation can be separated by calculation.

Upon heating or cooling a body in the transient method, an energy balance yields the following relation:

$$h A (t_o - t_a) = m c_p \frac{dt}{d\theta} \qquad \text{eqn. [1]}$$

where h is the combined heat transfer coefficient, A is the heat transfer area, c_p is the specific heat of the body, m is the mass of the body, t_o is the temperature at time zero, t_a is the temperature of the ambient, and θ is time.

If steady state exists at time zero, the equation can be integrated to:

$$\frac{t - t_a}{t_o - t_a} = e^{-\frac{hA}{m c_p}\theta} \qquad \text{eqn. [2]}$$

Solving for h:

$$h = \frac{m c_p}{A} \times \frac{1}{\theta} \ln\left(\frac{t_o - t_a}{t - t_a}\right) \qquad \text{eqn. [3]}$$

If corresponding values of the time and the temperature difference ratios are plotted on semi-log paper, the cooling (or heating) curve is obtained. For situations where the heat transfer coefficients are nearly constant with temperature difference, the data points plot as a straight line and the slope of this line is used in calculating the heat transfer

coefficients. Under conditions of variable conductance, equation three is still applicable provided the instantaneous slope at a particular time and its simultaneous temperature can be measured from the cooling curve, and fluid flow equilibrium exists.

In the present investigation, the heat transfer conductance is variable with time and is a maximum at the maximum temperature difference, i.e., at time zero. As the model cools down, flow inertia effects will exist, giving rise to higher heat transfer conductances than would exist under flow equilibrium conditions. This precludes the use of obtaining heat transfer coefficients from the lopes of the cooling curve other than at the initial or time zero point. Therefore, it is necessary to measure the slope at time zero in order to obtain the heat transfer coefficient that pertains at steady state.

The heat transfer coefficient obtained per equation three is the combined heat transfer coefficient,

$$h = h_c + h_r \qquad \text{eqn. [4]}$$

where h_c is the convective heat transfer coefficient and h_r is the radiation heat transfer coefficient.

For a gray body at temperature T_o and radiating to black surroundings at temperature T_a, the net radiant heat exchange is:

$$q_r = \epsilon \sigma A \left(T_o^4 - T_a^4 \right) \qquad \text{eqn. [5]}$$

where ϵ is the emissivity of the gray body and σ is the Stefan-Boltzman Constant.

This expression is applicable for surroundings that are not black provided the radiating body is so small that it intercepts only a negligible portion of the radiation reflected from the surroundings. Essentially, such conditions exist in the experimental apparatus when the heat source is

turned off.

Equation (5) can be expressed by an equivalent heat transfer coefficient by dividing through by A and (To - Ta), giving

$$h_r = \epsilon \sigma \left(T_o^2 + T_a^2 \right)\left(T_o + T_a \right) \qquad \text{eqn. [6]}$$

If the values of the emissivities of the test specimens are known, the heat transfer by radiation can be calculated.

5. Presentation of Results

Free convection heat transfer relationships are generally described in a dimensionless system in which Nusselt number is expressed as a function of Grashof and Prandlt number:

$$Nu = \phi (Gr, Pr)$$

In cases of simple geometry such as infinitely long cylinders, spheres, and plane surfaces, the length term in the Grashof number can easily be described by one dimension. For an infinitely long horizontal cylinder:

$$Nu = C \left(\frac{g \beta^2 \rho^2 \Delta t d^3}{\mu^2} \times \frac{\mu c_p}{k} \right)^m$$

where the characteristic dimension is d, the diameter of the cylinder.

The flat plates tested are presented in this form using the horizontal diameter (or edge length) as the significant dimension.

For more complex geometries, one or more dimensionless terms called shape factors must be introduced to insure geometric similarity between two systems. [5] Thus, for a horizontal cylinder of diameter, d, and axial length L, the free convection equation becomes:

$$Nu = C \left(\frac{g \beta^2 \rho^2 \Delta t d^3}{\mu^2} \times \frac{\mu c_p}{k} \right)^m \left(\frac{d}{L} \right)^n$$

As the geometry becomes more complex, it becomes more and more difficult to describe the geometry in terms of a shape factor. To date, results have been published for only a few relatively simple shapes such as cylinders of finite length, blocks, parallel plates, spaces enclosed by plane surfaces, and annuli [4].

Formulation of a shape factor for the screens tested was not justified

due to the limited types of specimens available.

In establishing dimensionless correlations, choice of a linear dimension is immaterial so long as it is completely defined, and is characteristic of the geometry under consideration. Results for the wire screens are presented using two different methods in describing the linear dimension. The first one uses the screen wire diameter as the significant length. This serves to compare the screens with each other and with a single horizontal cylinder of infinite length. The second method uses screen matrix diameters measured in the horizontal plane in order to compare them with solid flat plates.

6. Experimental Apparatus

Photographs and schematic drawings of the apparatus are shown in figures 16 to 19. The apparatus consisted essentially of a large rigid frame to support components, a reflector and lamp to provide radiant heat, a suspension rig to position specimens accurately, a shelf, with window, to isolate reflector disturbances from the specimen, a calibration stand for adjusting reflector beam pattern, and a reflecting pyramid to scatter unused beam energy.

Experimental rigor required that the following conditions be met:

(a) The heat source be isolated in such a manner that convective disturbances created by it are not seen by the test specimen.

(b) The heat flux be directed in such a way that it does not heat the specimen environs to any appreciable degree.

(c) The heat flux pattern must be so adjusted as to give uniform surface temperatures at steady state flow conditions.

(d) Disturbance factors created by supports, instrumentation, and the environment be reduced to the minimum.

The heat source was isolated completely by means of the shelf and window between the reflector and test specimen. The upper surface of the shelf was covered with aluminum foil to reflect stray radiation from the reflector. The under surface was painted with aluminum paint. The window consisted of a thin sheet of polyvinylidene chloride plastic. Glass was tried originally and rejected because it heated up excessively and cooled slowly. The plastic sheet had a high tranmissivity and a small

thermal capacity. Substitution of the plastic for glass was a major breakthrough. It permitted the specimen to be moved farther away from the floor. This reduced the problem of disturbances from underneath and at the same time permitted better utilization of beam energy.

The heat source consisted of a reflector and a General Electric 500 watt floodlight. This type of lamp was used because it had a closely packed filament. Original design called for the use of General Electric 500 watt industrial type infra-red lamps. These were rejected because their filaments were not concentrated enough to give a good focus. The reflector was a modified parabolic type with a focal length of 58 inches. The convergence-divergence feature of the beam permitted use of any size specimen between three and twelve inches merely by positioning the specimen at different locations along the axis of the beam.

The heat flux pattern was adjusted by two methods. Large changes were made by changing the position of the lamp. Final adjustments were made (with a calibration specimen in position) by masking off portions of the beam. Masking consisted of placing small aluminum strips at various places on the upper surface of the shelf window. By beam attenuation it was possible to reduce surface temperature differences of the specimen to the order of two or three degrees at maximum temperature.

Heat flux intensity was regulated by means of a variable voltage transformer.

Disturbance factors caused by the environment were reduced to an acceptable degree by providing a large test enclosure. Cold smoke tests showed that a chimney was being created by heating of the floor. This was corrected by the reflecting pyramid. Test instruments were enclosed in an insulated booth located apart from the test area. This served two purposes.

Instruments were kept at a constant temperature and the operator was given the freedom of motion necessary to take data.

Disturbance factors caused by support of the specimen were negligible. The specimens were supported only by eight find cotton threads. No insulators or clamps were attached to the specimen.

Parasitic heat losses consisted only of the very small heat loss via one pair of thermocouple leads. Thirty gage thermocouple wire was used to reduce this effect to a negligible value.

Instruments and elements used were:

(a) Leeds and Northrup Company Speedomax Recorder, Model G, serial 3661.

Range: 0-40 millivolts, Variable.

Sensitivity: 1/100 of a millivolt.

Response: Full scale in one second.

Chart Speed: Three inches per minute.

(b) Rubicon Precision Potentiometer, Model 2732, serial 96586

Range: 0-50 millivolts

Sensitivity: 5/1000 of a millivolt

(c) Thermocouples. One per specimen to measure temperature potential. One on each post of frame to measure ambient temperature.

(d) Mercury thermometer. Used as a reference to check thermocouple and instrument calibration.

7. Description of Specimens

Six test specimens, each instrumented with single thermocouples, were used to obtain heat transfer data:

Solid flat plate, square

Solid flat plate, round

60 x 60 mesh screen, round

24 x 24 mesh screen, round

16 x 16 mesh screen, round

10 x 10 mesh screen, round

Six calibration specimens were used to adjust the reflector beam pattern. These specimens were instrumented with five thermocouples; otherwise they were identical in all respects to the test specimens.

All thermocouples were iron-constantan, - wire size: 30 gage; insulation: fibre glass over cotton.

Detailed data for the plates and screens are listed in Table I.

8. Experimental Procedure

The time temperature history of each specimen, as it cooled from a heated equilibrium condition to ambient temperature, was recorded.

The first step was to achieve uniform temperature distribution over the specimen surface at steady state conditions. This was accomplished by placing a calibration specimen in test position and adjusting the beam pattern until all thermocouples indicated equal temperatures. Adjustment for uniform temperature was not easy, particularly with the screens. Flow through and across the screens was turbulent and oscillatory. Oscillations appeared to be completely random. Study was made of this by switching rapidly from one thermocouple channel to another. The temperatures were observed to converge and diverge as the main stream of flow shifted back and forth across the screen. Furthermore each adjustment to the beam pattern required about ten minutes of observation in order to evaluate its net effect.

The second step was to make several trial runs to check the general nature of the flow patterns. With experience, it was possible to anticipate when the flow would stabilize long enough to get a smooth run. An error in this respect still gave significant data but resulted in scattering.

In step three, the calibration specimen was removed and a test specimen placed in position. In all cases, the stability of flow improved remarkably. The calibration stand together with the multiple thermocouples of the calibration specimen evidently had induced extra turbulence.

Runs at several temperature levels were observed for each test specimen. Initial temperature of the specimen was controlled by varying

the voltage to the radiant heat source.

Upon completion of these runs, a mask was attached to the specimen. Runs were then repreated over the same temperature range and for approximately the same values of initial temperature.

The purpose of runs with the mask was to check for edge effects.

Data recorded were temperature of the specimen, ambient temperature, time, and atmospheric pressure. Such data are illustrated in tables II to VII.

9. Discussion of Results

In Figure 1, the convective heat transfer coefficients are shown for a square plate instrumented by one thermocouple with leads dropping straight to the floor and a similar plate instrumented by nine thermocouples with fifteen inch leads dropping to the calibration stand. The thermocouple leads and test stand are shielded from direct radiation by the plate.

According to Fischenden and Saunders [5], the convective heat transfer from the under surface of a horizontal plate should be non existent unless flow is precipitated by external causes or by temperature variations on the surface of the plate. Figure 1 shows the influence of increased disturbances on the lower side of the plate. The disturbances created by the test stand did increase the heat transfer coefficient of the plate. Since there is no reason to believe that the heat transfer from the upper surface should change, the increase in heat transfer was due to an increase from the lower surface. The difference in heat transfer coefficients for the two sets of conditions is about 12%.

In Figure 2, the same type of comparison is made. In this situation, the calibration stand receives direct radiation because of the porosity of the screen. The effects of the disturbance are greatest at low temperature potential. The error introduced at a temperature potential of 60 degrees is about 60%. At a temperature difference of 125 degrees, the error is about 20%.

Figures 1 and 2 emphasize most emphatically the necessity for keeping the free convection test environment "clean". For all test specimens the leads to the single thermocouples were dropped straight to the floor. The extension wire was carefully wrapped with aluminum foil to reflect

incident radiation.

In the investigation of the convective heat transfer characteristics of plates and screens, the specimens used should be very large in the horizontal dimension. Practically, from considerations of the size of enclosure, specimen support, and radiant power required, a compromise must be made. The size of 6.3 inches was used because it was the maximum size for the radiative power available and was considered large enough to minimize edge effects. The procedure adopted was to proceed with the investigation using this size as a standard and using a mask to check edge effects.

The mask was a thin sheet of insulating board three feet in diameter with the upper surface covered with aluminum foil. The center section had a 6.3" by 6.3" aperature to accommodate the square flat plate, and was modi- to a 6.3" diameter when necessary to accommodate the round test specimens. Thin strips of masking tape applied on the under side were used to seal the specimen edges to the mask.

Figures 3 through 7 show the results of these tests. For the flat plate an error of about 3.5% is introduced due to edge effects. The errors for the 60 x 60 screen and the 24 x 24 screen were not significant. The plot for the 16 x 16 screen shows a small divergence between the two curves at maximum temperature potential. The maximum error appears to be about 4% which is still within acceptable limits.

Figure 7, for the 10 x 10 screen shows a surprising result. It would seem that the greater the porosity, the less the effects of edges. The data for these runs however, indicate the higher the porosity, the larger the edge effect.

Figure 8 shows a plot of Nu versus Gr Pr for both the round flat plate and the square flat plate. Results of previous work by Fischenden and Saunders are also shown. For complete agreement, the data points should lie midway between the upper and lower curves reported by Fischenden and Saunders. Quantatively the values of the Nusselt numbers are about 6.4% below the mid line. In values of the heat transfer coefficient the difference amounts to about 20%.

Figures 9 through 12 show Nu versus Gr Pr for the four screens tested with screen wire diameter as the linear dimension in Nu and Gr Pr.

Figure 13 is a plot of Nu versus Gr Pr for all specimens using horizontal matrix diameter as the linear dimension. This graph compares the heat transfer characteristics of the screens to flat plates of equivalent size.

Figure 14 shows Nu versus Gr Pr for the screens based on screen wire diameters, together with McAdams' [3] curve for an infinitely long horizontal cylinder. The curves for the four screens appear to follow a definite pattern. Unfortunately, the range of data for the various screens is too limited to generalize. The slope of the 10 x 10 screen is not in consonance with the slope trends of the other three screens.

10. Conclusions

1. A transient testing technique has been developed for determining the convective heat transfer coefficients for solid flat plates and wire screen matrices under conditions of free-horizontal suspension.

2. Free convection heat transfer coefficients for single, horizontal, wire screen matrices have been determined for the ranges of Grashof-Prandtl number listed in Tables IV through VII.

3. Edge effects were investigated and found to be of small magnitude except for the 10 x 10 screen.

4. Figure 14 indicates that a relationship to correlate data for all single wire screen matrices in horizontal free convection might exist. More data using additional screens and covering a greater range of Grashof number are needed to confirm or refute this opinion.

11. Recommendations for Future Work

(a) Additional data is necessary to extend the range of Grashof numbers. A screen size of about 40 x 40 meshes to the inch is needed to fill the gap between the 24 x 24 and 60 x 60 screens. Data for a screen size of 5 x 5 meshes per inch are required also to complete the comparison with a horizontal cylinder. Large heating powers are needed for a 5 x 5 screen. The heat source in this investigation did not have sufficient strength to heat the 5 x 5 screen.

(b) It is believed the apparatus developed can be used to determine emissivities. The test procedure would consist of electroplating a specimen with cadmium or other metallic film for which the emissivity is accurately known. By testing this specimen and a similar uncoated specimen under identical test conditions, the heat transfer coefficients of convection and radiation could be separated and the emissivity of the uncoated specimen calculated.

12. Bibliography

1. J. E. Coppage, "Heat Transfer and Flow Friction Characteristics of Porous Media", Technical Report No. 16, Navy Contract N6-ONR-251 Task Order 6, Stanford University, 1 December 1952.

2. F. T. Rogers, Jr., and H. L. Morrison, "Remarks on the Theory for Convection in Porous Media", 1951 Heat Transfer and Fluid Mechanics Institute, Preprints of Papers, Stanford University, 20 June 1951.

3. W. H. McAdams, "Heat Transmission", Third Edition, McGraw-Hill Book Co., Inc., New York, 1954.

4. Max Jakob, "Heat Transfer", Volume 1, John Wiley & Sons, Inc., New York, 1949.

5. M. Fischenden and O. A. Saunders, "An Introduction to Heat Transfer", Oxford Press, 1950.

6. R. Weise, "Forschung a.d. Geb. d. Ingenieurwes", 6, 281, 1935.

7. C. R. Garbert, "The Transient Method for Determining Heat Transfer Conductance From Bodies in High Velocity Flow", Heat Transfer and Fluid Mechanics Institute Preprint of Papers, Stanford University, 20 June, 1951.

8. W. H. Geidt, "Principles of Engineering Heat Transfer", Second Edition, D. Van Nostrand Co., New York, August, 1957.

9. M. Jakob and W. Linke, "Forschung a. d. Geb d. Ingenieurwes", 4, 75, 1933.

10. W. Nusselt, "Zeitschr d. Ver. deutsch. Ing.", 73, 1475, 1929.

11. A. H. Davis, "Phil". Mag (6) 44, 920; 1922.

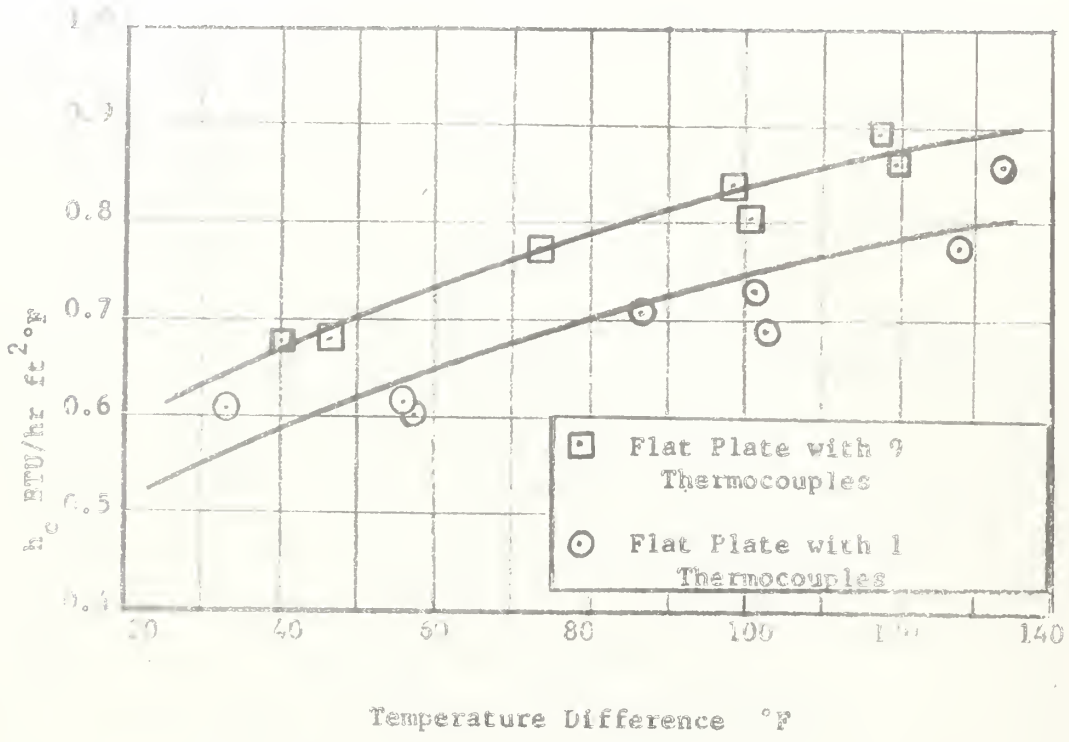

Figure 1: Increase in Convective Heat Transfer for Flat Plate due to Disturbing Influence of the Calibration Stand and Multiple Thermocouple Attachments.

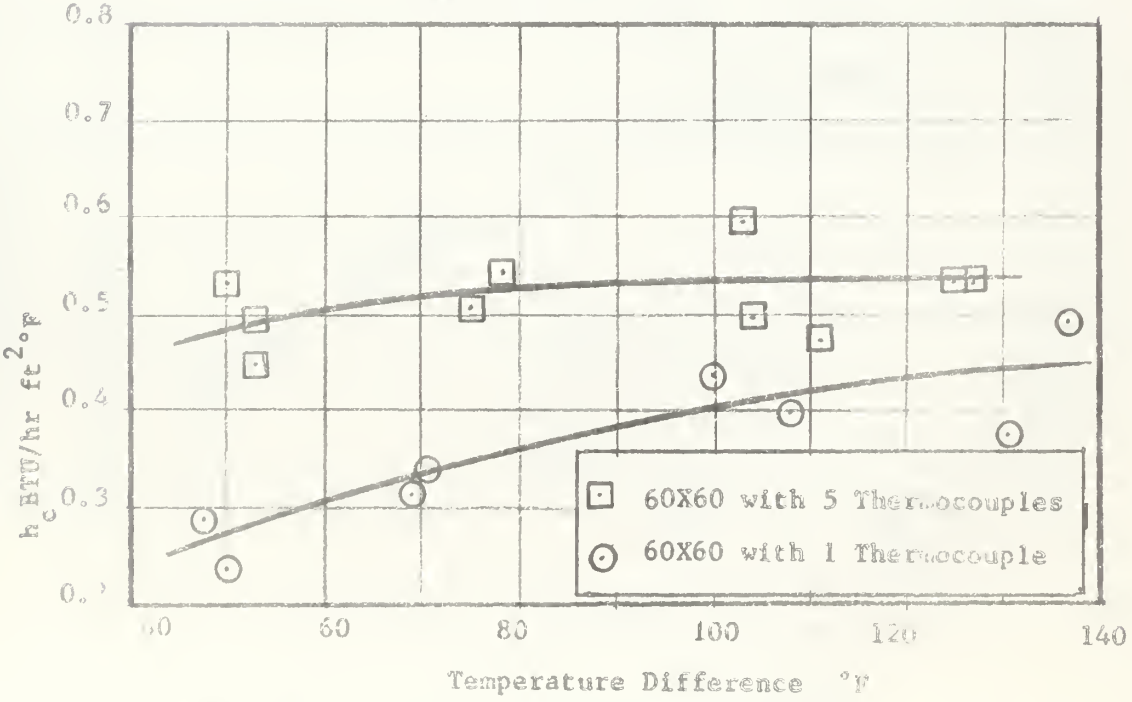

Figure 2: Increase in Convective Heat Transfer for 60 X 60 Screen due to Disturbing Influence of the Calibration Stand and Multiple Thermocouple Attachments.

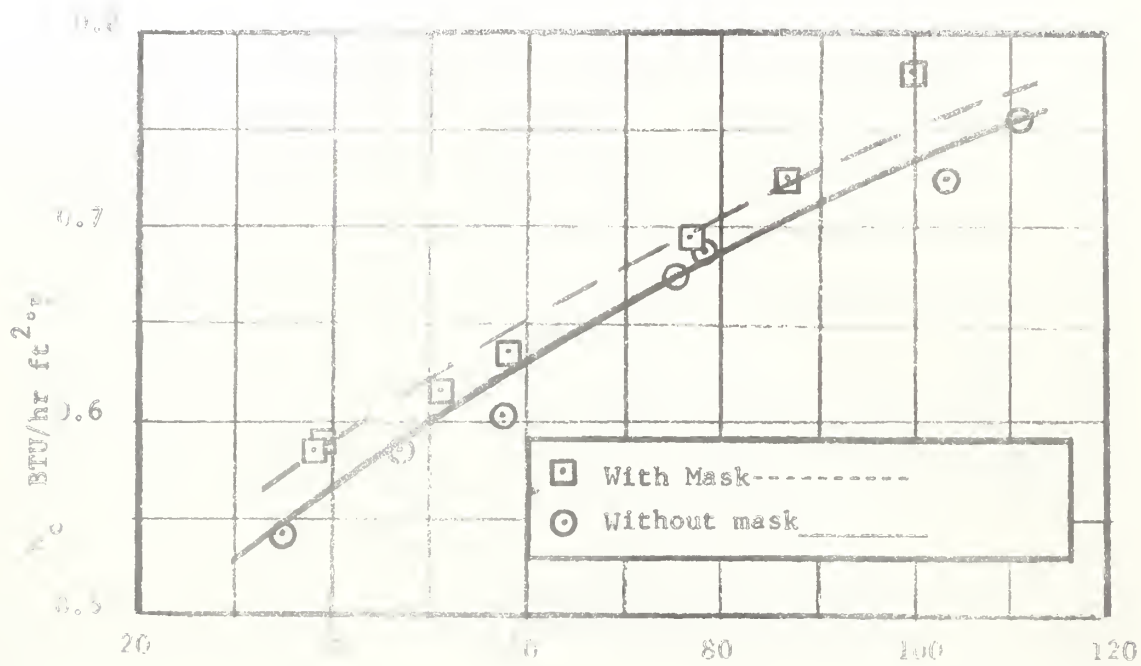

Figure 3. Free Convection Edge Effects
6.3" Square Flat Plate

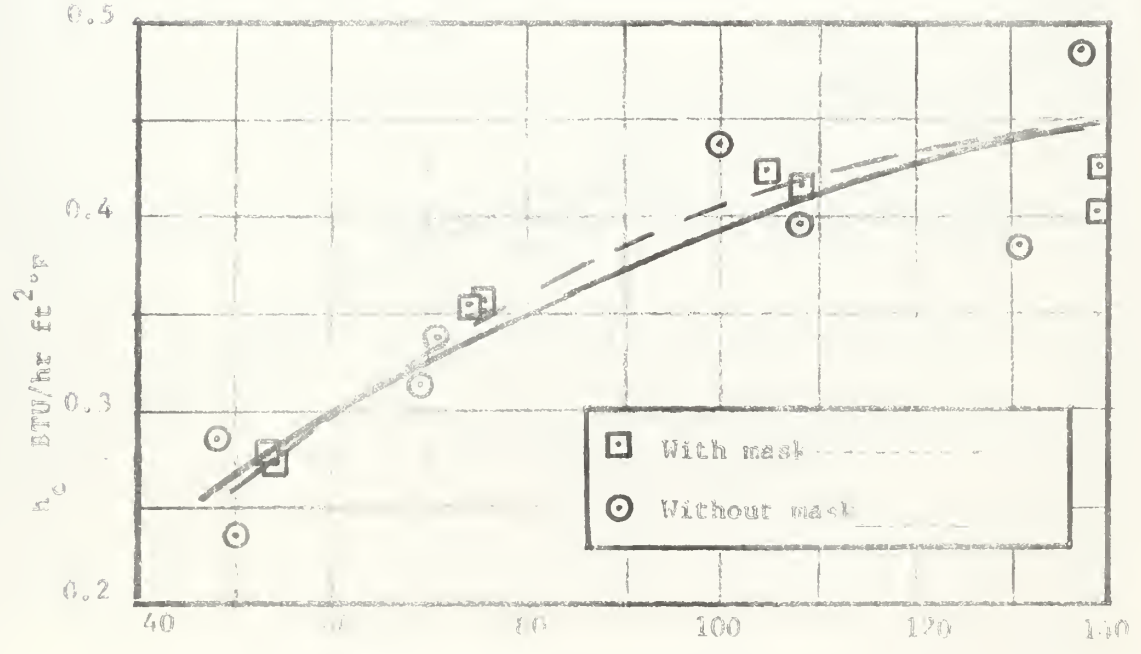

Figure 4. Free Convection Edge Effects
6.3" Diameter 60 x 60 Screen.

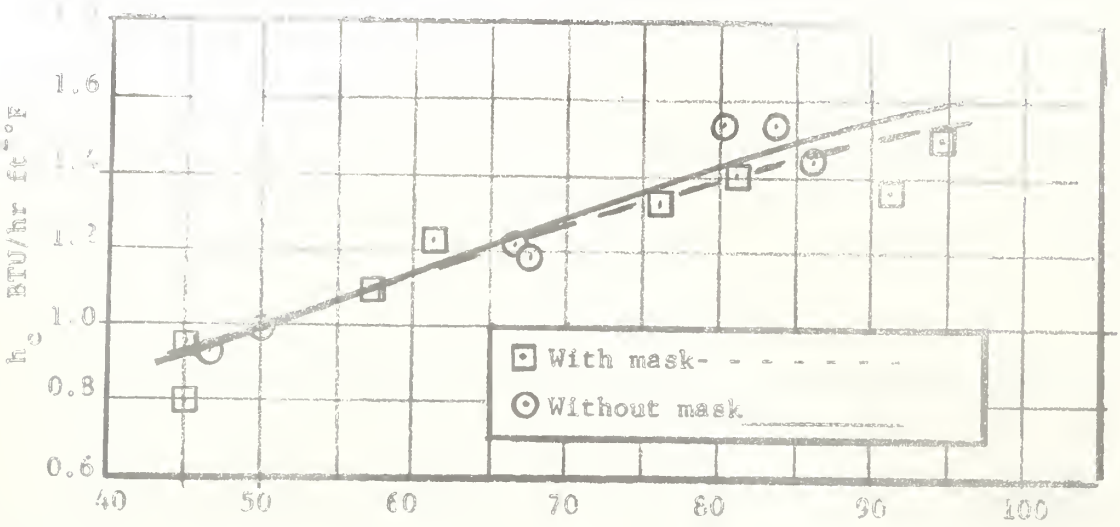

Temperature Difference °F

Figure 5. Free Convection Edge Effects
6.3" Diameter 24 x 24 Screen.

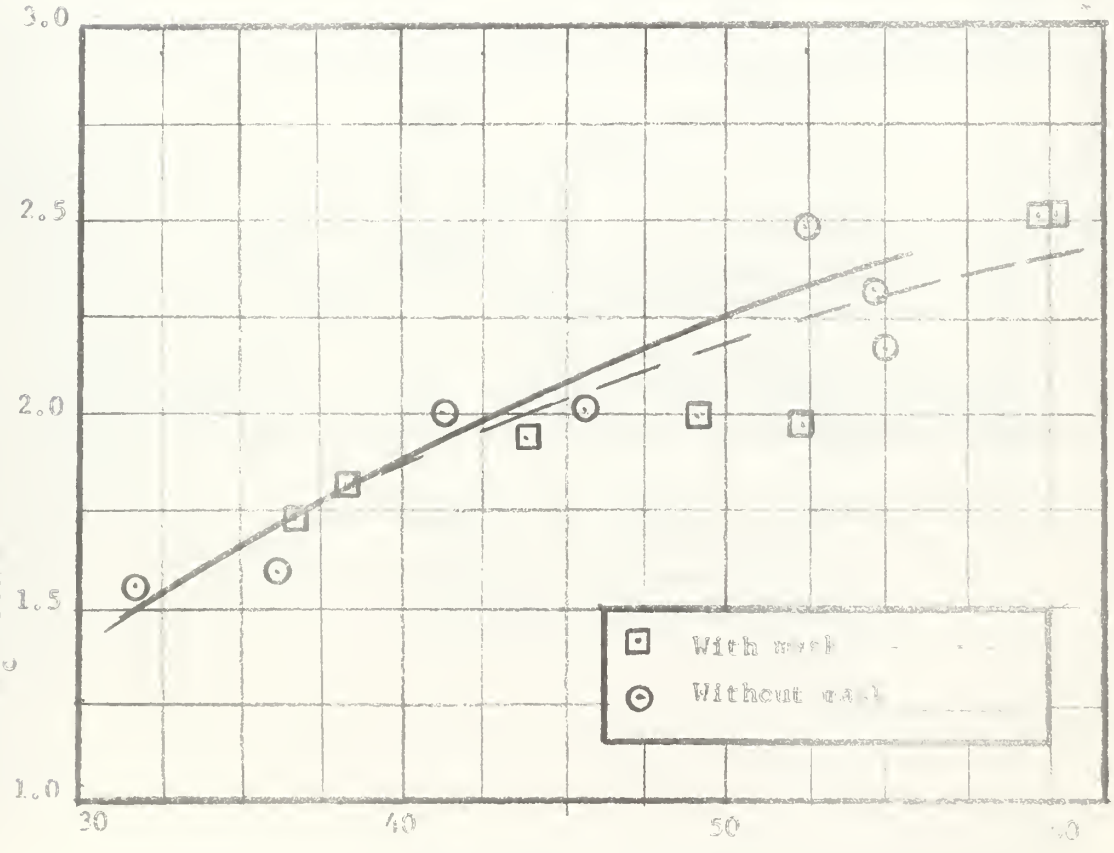

Temperature Difference °F

Figure 6. Free Convection Edge Effects
6.3" Diameter 16 x 16 Screen.

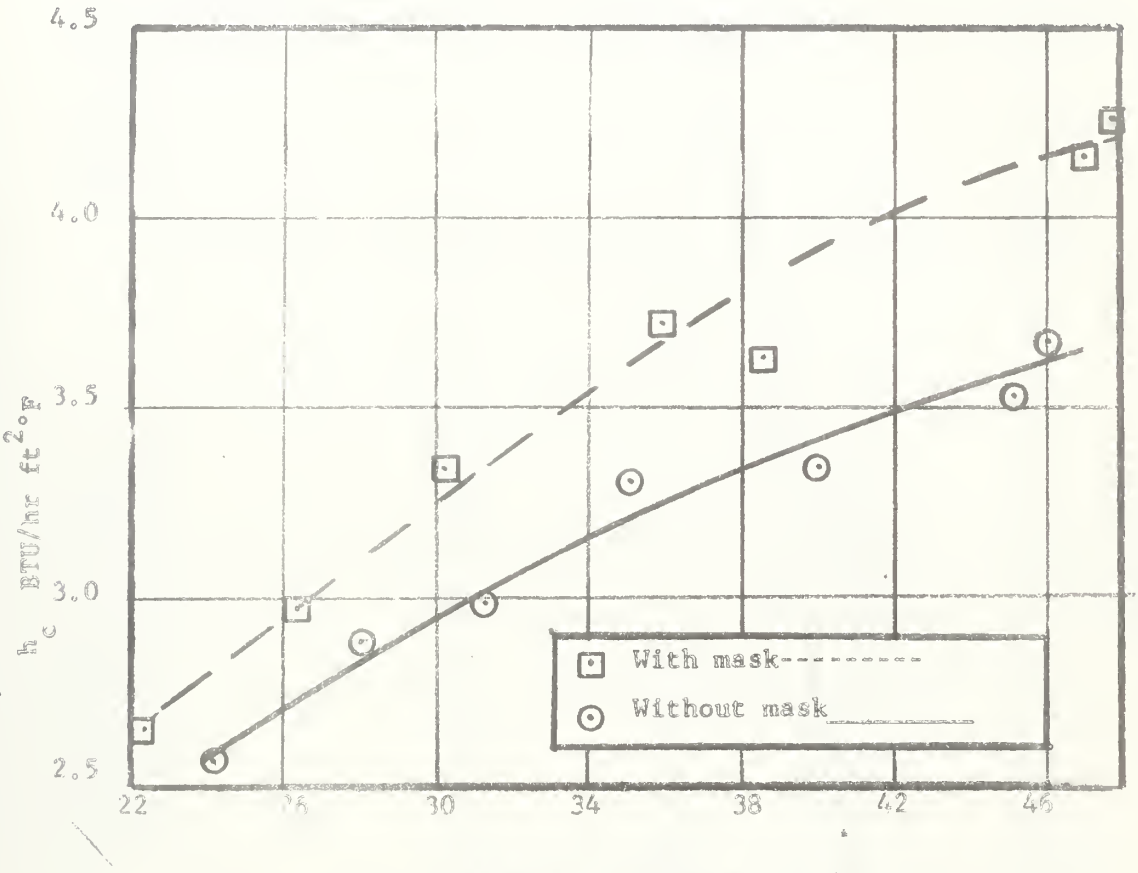

Figure 7: Free Convection Edge Effects
6.3" Diameter 10 x 10 Screen.

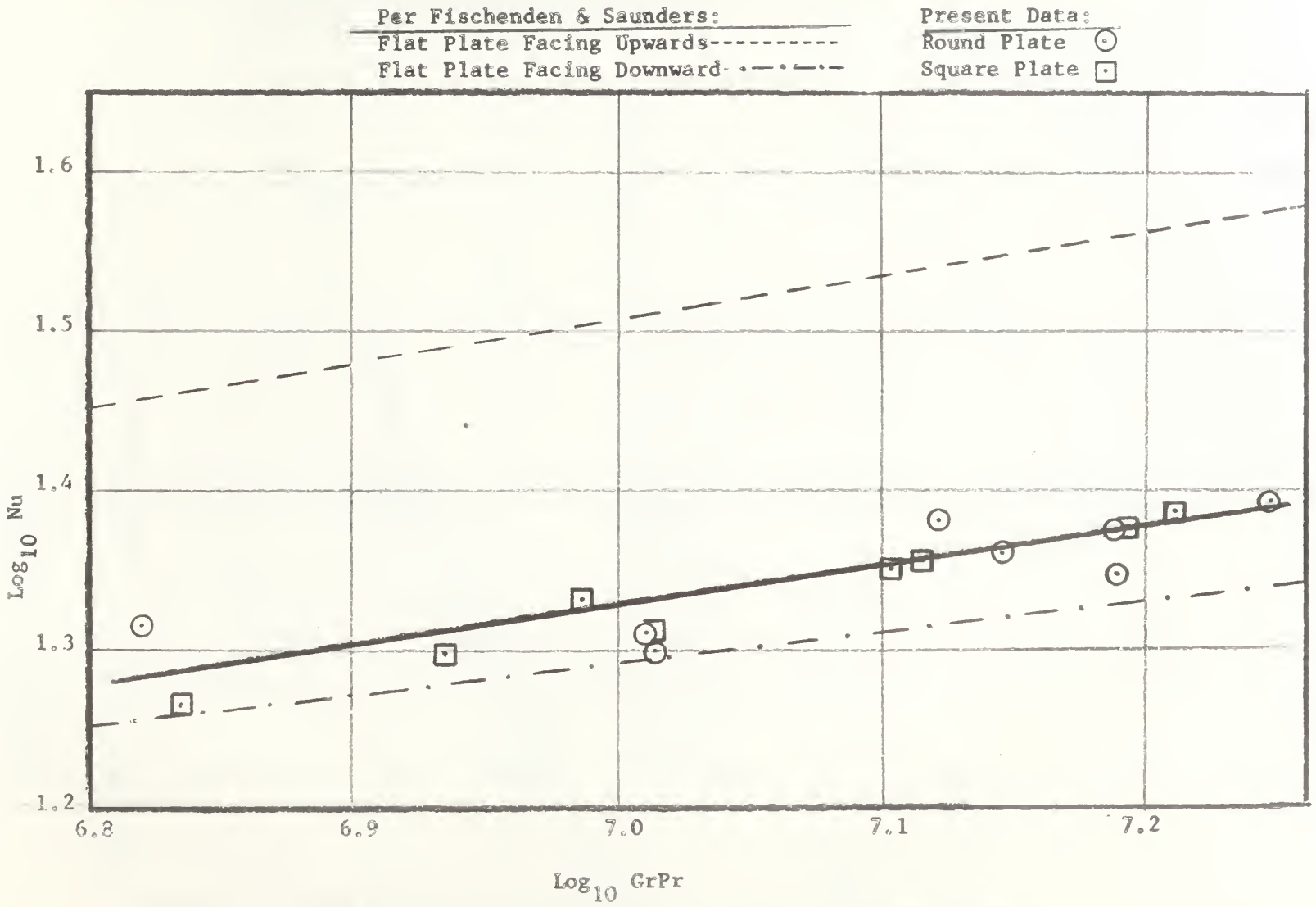

Figure 8: Log Nu vs Log GrPr for 6.3" Flat Plates

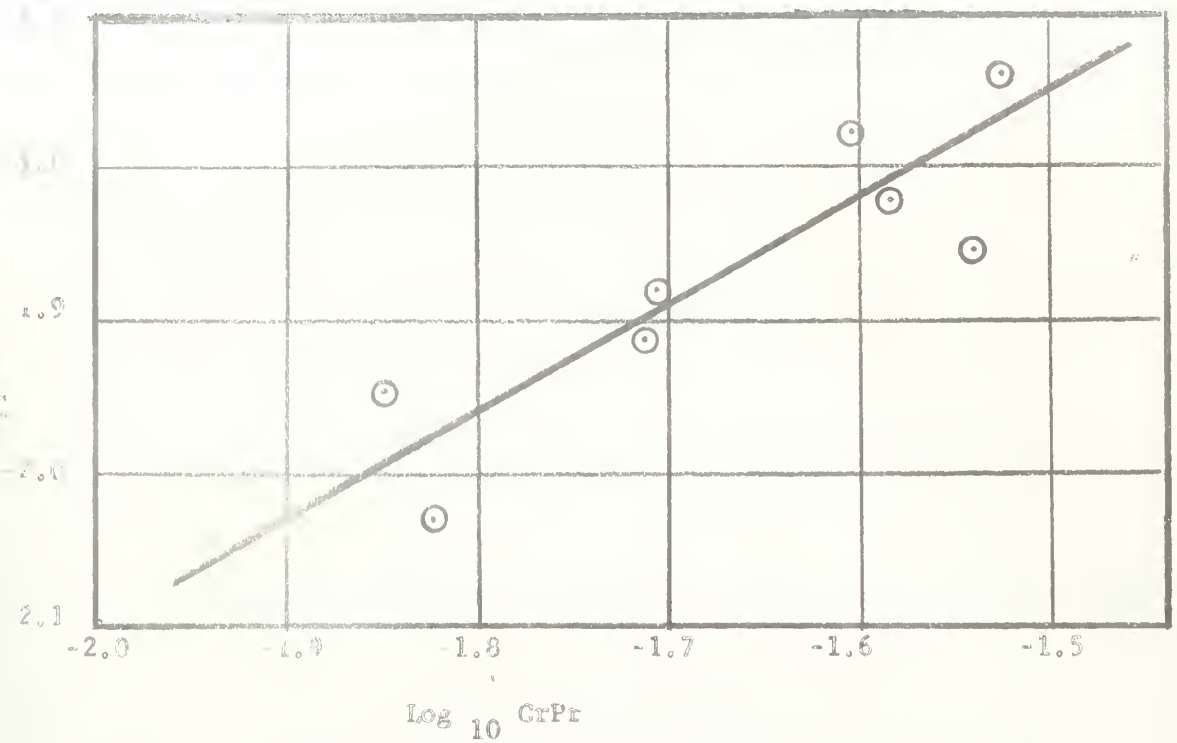

Figure 9: Log Nu vs Log GrPr for 60 x 60 Screen
Significant Dimension is Screen Wire
Diameter.

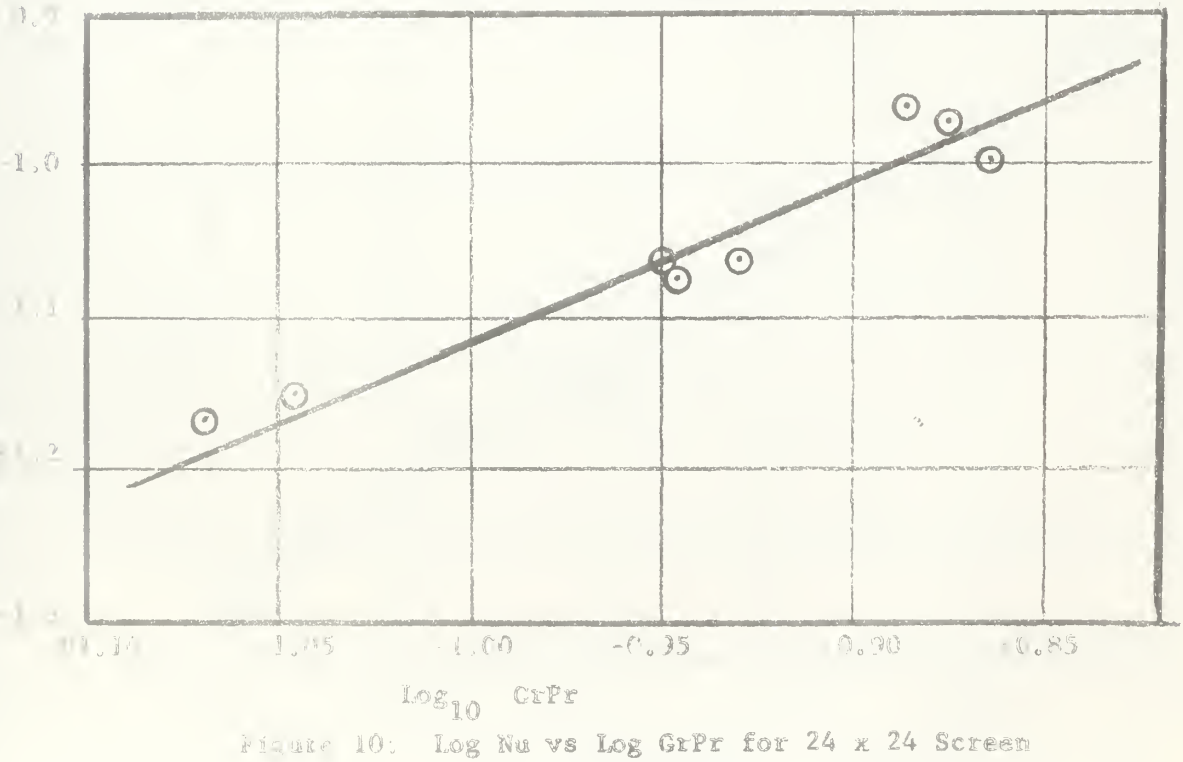

Figure 10: Log Nu vs Log GrPr for 24 x 24 Screen
Significant Dimension is Screen Wire
Diameter

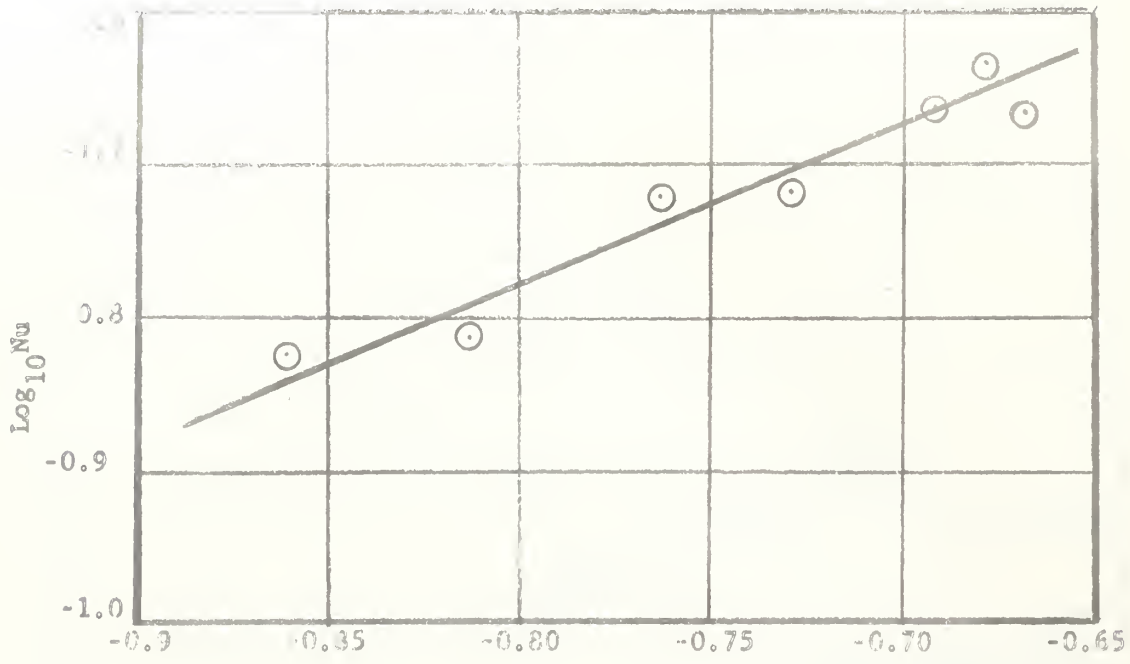

Figure 11: Log Nu vs Log GrPr for 16 X 16 Screen Significant Dimension is Screen Wire Diameter.

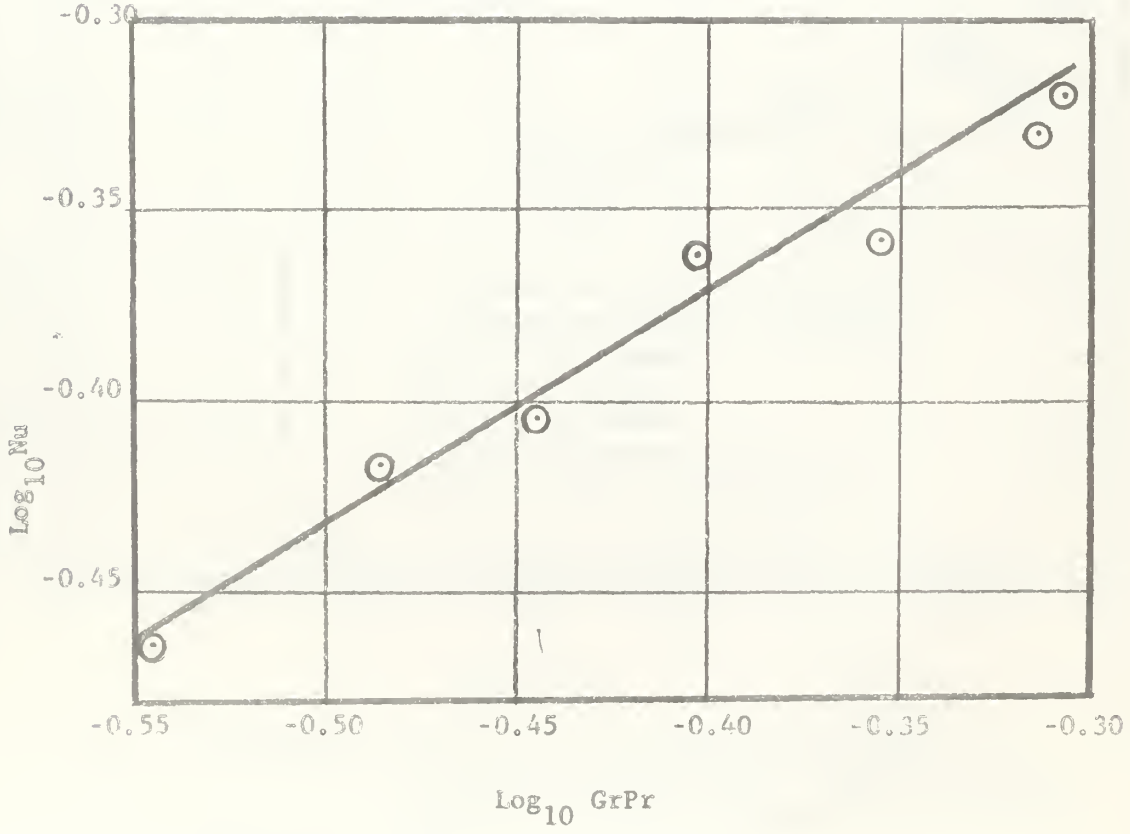

Figure 12: Log Nu vs Log GrPr for 10 X 10 Screen. Significant Dimension is Screen Wire Diameter.

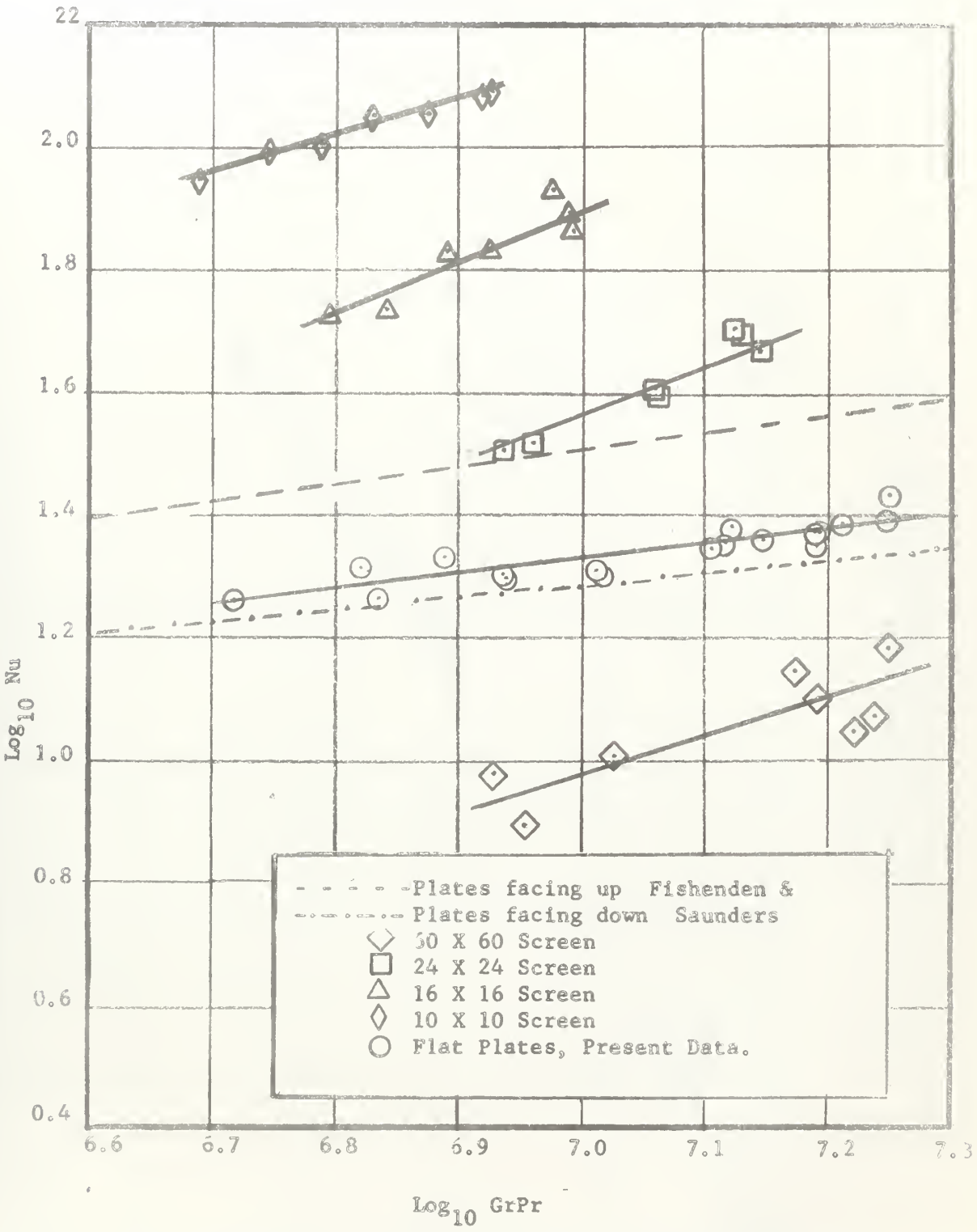

Figure 13: Log Nu vs Log GrPr for Flat Plates and Screens using Horizontal Plate and Screen Diameters as the Significant Linear Dimension

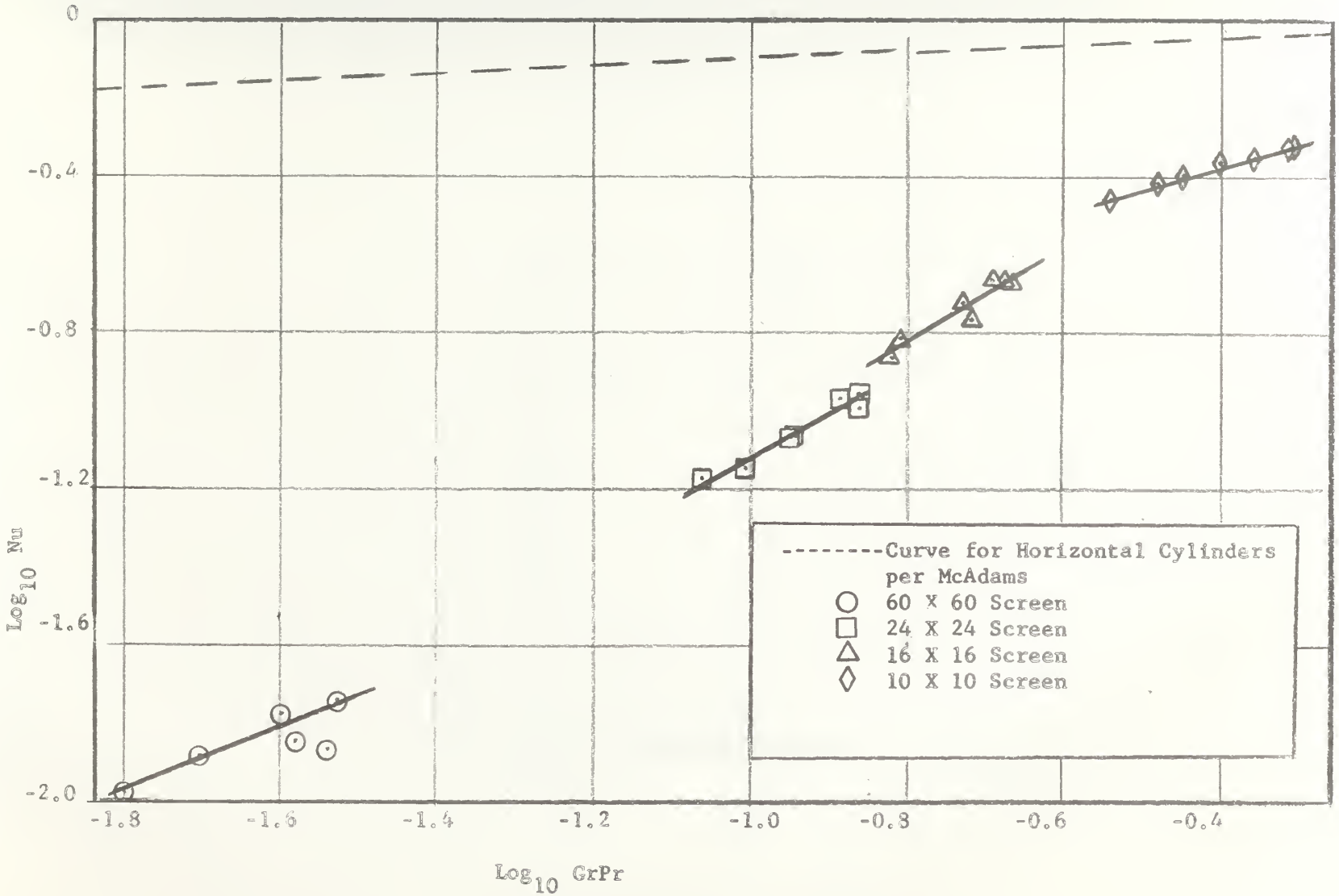

Figure 14: Log Nu vs Log GrPr for Wire Screens Using Wire Diameter as the Significant Dimension.

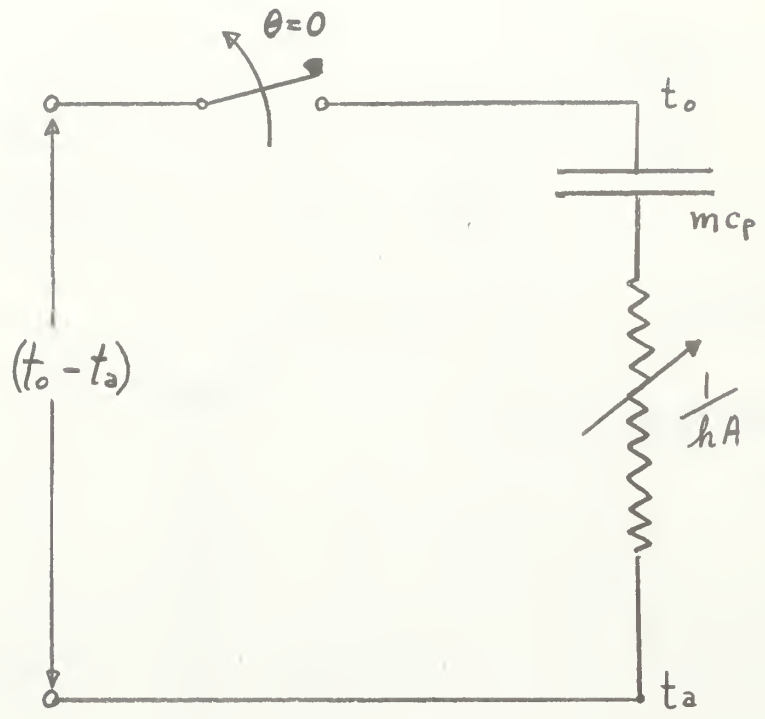

Figure 15: Thermal Circuit Shown above is analogous to Electrical Resistance Capacitance Circuit.

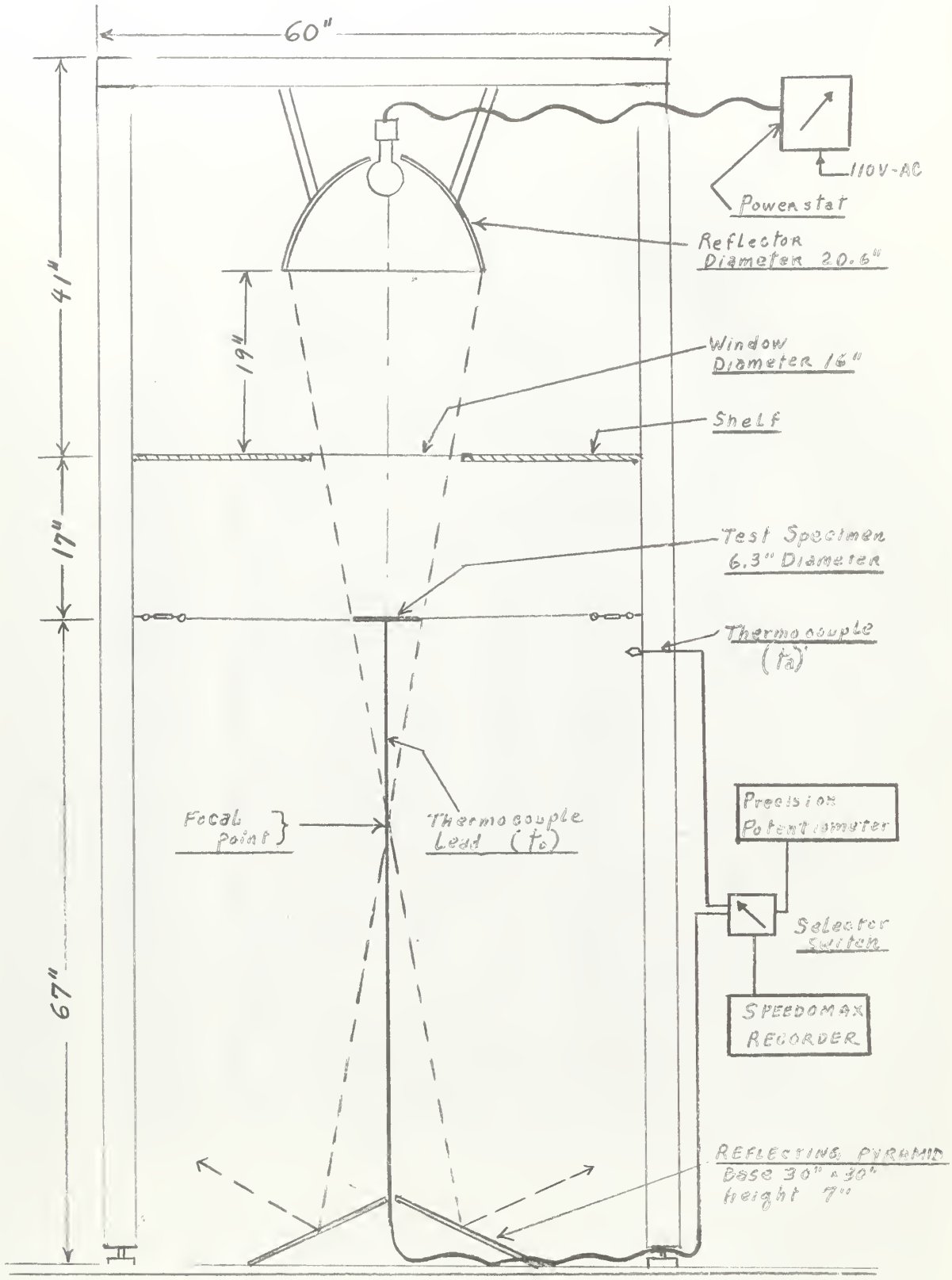

Figure 16: Diagram of Experimental Apparatus Showing Principal Components and Dimensions.

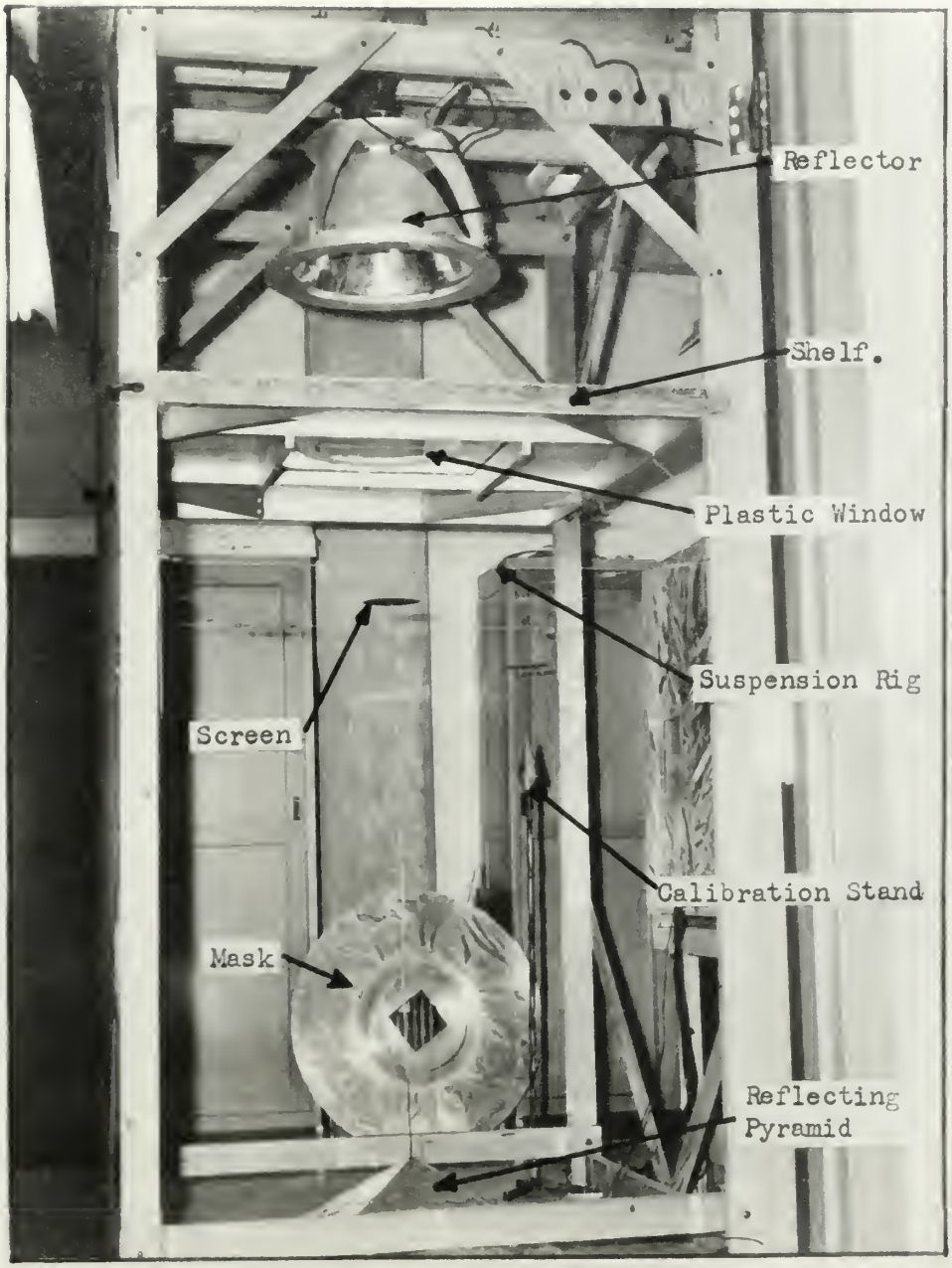

Figure 17: Experimental Apparatus. Main frame and components are shown. Operator's booth can be seen to the right of the main frame.

Figure 18: Reflector, lamp, and some of the test and calibration specimens are shown.

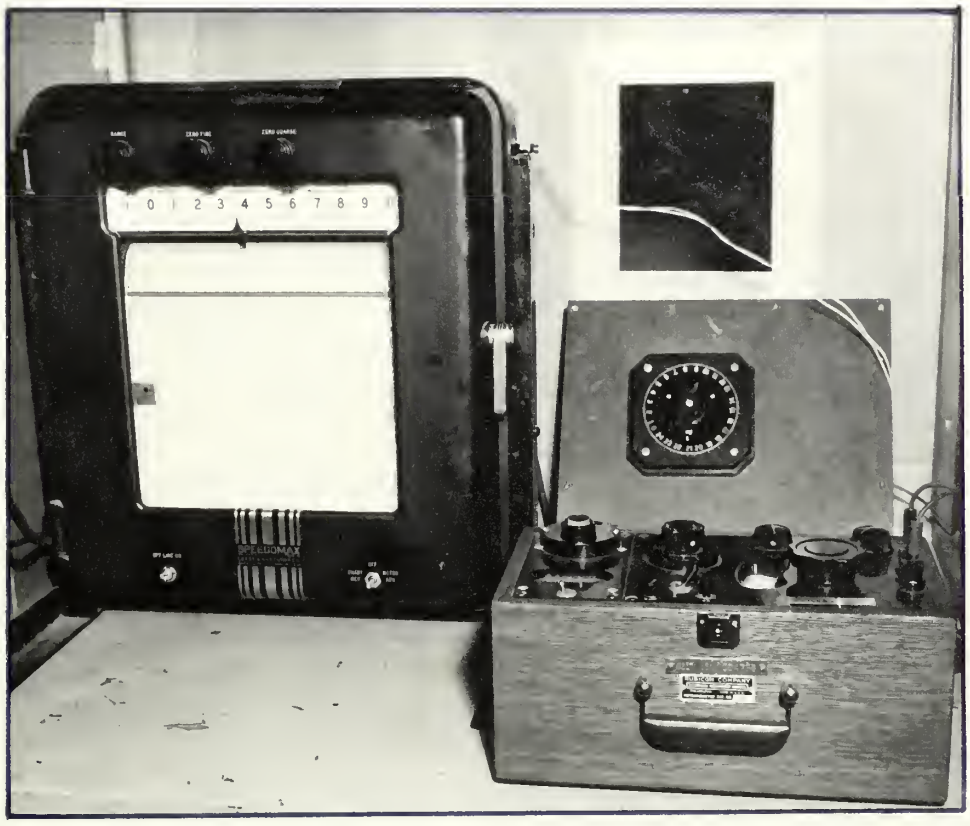

Figure 19: Photograph shows interior of Operator's Booth. Shown are the Leeds and Northrup Speedomax Recorder, the Rubicon Precision Potentiometer, and selector switch. Window for monitoring test area is shown in the background.

TABLE I

DETAILS OF PLATES AND SCREENS

Specimen & Description	Flat Plates		Wire Screens			
	Square	Round	60x60	24x24	16x16	10x10
Diameter(in)		6.3	6.3	6.3	6.3	6.3
Length(in)	6.3					
Meshes/inch	--	--	60x60	24x24	16x16	10x10
Nominal Wire Diameter(in)	--	--	0.0075	0.0140	0.0180	0.025
Actual Wire Diameter(in)	--	--	0.0075	0.0135	0.0177	0.0245
Thickness(in)	0.010	0.010	0.0145	0.0305	0.033	0.049
Mass(lbm)	0.134	0.1054	0.0456	0.0658	0.0705	0.0857
Porosity	0	0	0.675	0.725	0.766	0.817
Heat Transfer Area A_s,(ft^2)	0.551	0.435	0.680	0.463	0.403	0.344

NOTE: For plates, material is commerical copper, specific heat 0.093 BTU/lbm°F; thermal conductivity 222 BTU/hr ft°F; emissivity 0.10.
For all screens, material is 18/8 stainless steel, specific heat 0.12 BTU/lbm F; thermal conductivity 10 BTU/hr ft F; emissivity 0.25.

TABLE II

HEAT TRANSFER DATA

Square Flat Plate 6.3" x 6.3" x 0.010"

Run	to °F	ta °F	Slope at time zero l/hr	h $\frac{BTU}{hr\ ft^2\ °F}$	h_r $\frac{BTU}{hr\ ft^2\ °F}$	h_c $\frac{BTU}{hr\ ft^2\ °F}$	Nu	Gr Pr $\times 10^{-7}$
1	110.5	75.7	29.0	0.656	0.115	0.541	18.4	0.683
2	128.4	75.3	33.5	0.757	0.121	0.636	21.4	0.971
3	132.8	75.3	32.2	0.727	0.122	0.605	20.3	1.035
4	150.6	75.2	35.6	0.805	0.129	0.676	22.3	1.270
5	153.4	75.0	36.2	0.819	0.130	0.689	22.7	1.300
6	178.7	75.2	38.3	0.866	0.139	0.727	23.5	1.555
7	185.6	75.2	39.8	0.900	0.142	0.758	24.3	1.620
8	126.0	78.8	30.9	0.707	0.122	0.585	19.7	0.860

TABLE III

HEAT TRANSFER DATA

Round Flat Plate — 6.3" diameter x 0.010" thick

Run	to °F	ta °F	Slope at time zero 1/hr	h $\frac{BTU}{hr\ ft^2 °F}$	h_r $\frac{BTU}{hr\ ft^2 °F}$	h_c $\frac{BTU}{hr\ ft^2 °F}$	Nu	Gr Pr $x10^{-7}$
1	107.8	74.8	31.9	0.717	0.114	0.603	20.6	0.661
2	132.1	75.0	31.6	0.714	0.122	0.592	19.8	1.037
3	131.8	75.2	32.2	0.728	0.122	0.606	20.4	1.025
4	162.2	75.3	36.5	0.835	0.133	0.702	22.9	1.395
5	156.1	75.7	38.0	0.859	0.131	0.728	23.9	1.320
6	178.2	75.5	36.5	0.826	0.139	0.687	22.2	1.545
7	176.1	75.0	38.3	0.865	0.38	0.727	23.5	1.540
8	203.8	76.0	40.9	0.925	0.150	0.775	24.6	1.763
9	209.6	76.0	44.6	1.010	0.152	0.858	27.1	1.785

TABLE IV

HEAT TRANSFER DATA

Screen, 60 x 60 Meshes/in. 6.3" Diameter Porosity 0.675

Run	to °F	ta °F	Slope at time zero hr^{-1}	h $\frac{BTU}{hr\ ft^2\ °F}$	h_r $\frac{BTU}{hr\ ft^2\ °F}$	h_c $\frac{BTU}{hr\ ft^2\ °F}$	Nu(1) $\times 10^2$	$GrPr_2$(1) $\times 10^2$	Nu(2)	GrPr(2) $\times 10^{-7}$
1	210.3	79.7	94.3	0.766	0.383	0.377	1.40	2.88	11.75	1.72
2	217.0	79.7	108.1	0.877	0.390	0.487	1.81	2.98	15.22	1.78
3	187.0	79.3	93.2	0.757	0.360	0.397	1.51	2.61	12.65	1.55
4	179.5	79.3	97.6	0.792	0.354	0.438	1.67	2.49	14.02	1.49
5	149.9	79.3	81.9	0.665	0.327	0.338	1.32	1.96	11.10	1.17
6	148.5	79.3	78.4	0.637	0.325	0.312	1.22	1.93	10.20	1.05
7	129.0	79.3	66.8	0.543	0.308	0.235	0.935	1.50	7.85	0.895
8	126.9	79.3	73.0	0.592	0.306	0.286	1.13	1.31	9.50	0.845

(1) Based on wire diameter (2) Based on screen diameter

TABLE V

HEAT TRANSFER DATA

Screen, 24 x 24 Meshes/in. 6.3" Diameter Porosity: 0.725

Run	to °F	ta °F	Slope at time zero 1/hr	h $\frac{BTU}{hr\ ft^2 °F}$	h_r $\frac{BTU}{hr\ ft^2 °F}$	h_c $\frac{BTU}{hr\ ft^2 °F}$	Nu(1) x10^2	GrPr(1) x10^2	Nu(2)	GrPr(2) x10^{-7}
1	122.4	75.9	72.2	1.234	0.299	0.935	6.81	8.50	31.8	0.865
2	125.2	76.0	75.0	1.282	0.302	0.980	7.07	9.00	33.0	0.915
3	143.0	76.5	89.7	1.535	0.318	1.217	8.63	11.23	40.3	1.142
4	143.9	76.7	87.7	1.500	0.319	1.181	8.40	11.32	39.2	1.152
5	155.0	74.7	109.4	1.870	0.327	1.543	10.85	13.02	50.7	1.329
6	158.6	75.0	109.2	1.865	0.331	1.534	10.72	13.35	50.0	1.361
7	161.2	75.0	103.4	1.770	0.333	1.437	10.05	13.65	46.9	1.395

(1) Based on wire diameter (2) Based on screen diameter

TABLE VI

HEAT TRANSFER DATA

Screen, 16 x 16 Meshes/in — 6.3" Diameter — Porosity: 0.766

Run	to °F	ta °F	Slope at time zero 1/hr	h $\frac{BTU}{hr\ ft^2\ °F}$	h_r $\frac{BTU}{hr\ ft^2\ °F}$	h_c $\frac{BTU}{hr\ ft^2\ °F}$	Nu(1) x10	GrPr(1) x10	Nu(2)	GrPr(2) $x10^{-6}$
1	109.2	77.5	87.7	1.850	0.290	1.56	1.495	1.375	53.2	6.21
2	118.8	77.5	108.9	2.30	0.297	2.00	1.890	1.725	67.2	7.78
3	130.2	77.8	132.5	2.79	0.308	2.48	2.32	2.09	85.5	9.43
4	132.3	77.8	125.0	2.63	0.309	2.32	2.16	2.15	77.3	9.73
5	132.8	78.0	117.8	2.48	0.310	2.17	2.03	2.17	72.2	9.81
6	123.7	78.0	105.0	2.31	0.302	2.01	1.910	1.865	67.6	8.42
7	114.2	78.0	89.4	1.88	0.294	1.59	1.515	1.535	53.8	6.93

(1) Based on wire diameter

(2) Based on screen diameter

TABLE VII

HEAT TRANSFER DATA

Screen, 10 x 10 Meshes/in — 6.3" Diameter — Porosity: 0.817

Run	to °F	ta °F	Slope at time zero 1/hr	h_r BTU/hr ft^2°F	h_c BTU/hr ft^2°F	h BTU/hr ft^2°F	Nu(1) x10	GrPr(1) x10	Nu(2)	GrPr(2) x10^{-6}
1	109.2	77.5	87.7	1.85	0.290	1.56	1.495	1.375	53.2	6.21
2	118.8	77.5	108.9	2.30	0.297	2.00	1.890	1.725	67.2	7.78
3	130.2	77.8	132.5	2.79	0.308	2.48	2.30	2.09	85.5	9.43
4	132.3	77.8	125.0	2.63	0.309	2.32	2.16	2.15	77.3	9.73
5	132.8	78.0	117.8	2.48	0.310	2.17	2.03	2.17	72.2	9.81
6	123.7	78.0	105.0	2.31	0.302	2.01	1.910	1.865	67.6	8.42
7	114.2	78.0	89.4	1.88	0.294	1.59	1.515	1.535	53.8	6.93

(1) Based on wire diameter

(2) Based on Screen diameter

APPENDIX I

Probable Uncertainties

The probable uncertainties for measured and tabulated values used in this investigation are tabulated below:

Table of Probable Uncertainties

Item		Estimated Error
(1)	Thermocouples	± 1.5%
(2)	Rubicon Precision Potentiometer	± 0.075%
(3)	Speedomax Recorder	± 2.0%
(4)	Chart Time	± 2.5%
(5)	(to - ta) (5.0 mv)	± 2.5%
(6)	(t - ta)	± 2.5%
(7)	$\frac{(to-ta)}{(t-ta)}$	± 3.5%
(8)	$\frac{1}{\theta}$ in $\frac{(to-ta)}{t-ta}$	± 6.2%
(9)	$\frac{mc}{A}$	± 3.5%
(10)	h	± 7.5%
(11)	t	± 9.0%
(12)	h_r	± 20.0%
(13)	h_c :Plates	± 8.0%
	60x60	± 11.0%
	24x24	± 8.0%
	16x16	± 8.0%
	10x10	± 8.0%
(14)	Gr Pr	± 10.4%
(15)	Nu:Plates	± 8.0%
	60x60	± 11.0%
	24x24	± 8.0%
	16x16	± 8.0%
	10x10	± 8.0%

APPENDIX II

SAMPLE CALCULATIONS RUN K-7

From Table I

10 x 10 Mesh Screen — Diameter: 6.3 inches

Wire diameter: 0.0245 inches — Mass: 0.0857 *lbm*

Porosity: 0.817 — Heat Transfer Area: 0.344

Emissivity: 0.25 — Specific Heat: 0.12 BTU/lbm°F

Equation 3 applies

Setting up table from recorder chart (Figure II-1)

to = 2.60 mv. = 122.7°F — ta = 1.322 mv. = 78.7°F

Time (sec)	t (mv)	t-ta (mv)	$\frac{to-ta}{t-ta}$
0	2.600	1.278	1.000
5	2.380	1.058	1.208
10	2.203	.881	1.450
15	2.058	.746	1.713
20	1.958	.636	2.010
25	1.872	.550	2.322
30	1.804	.482	2.650
35	1.752	.430	2.970
40	1.667	.345	3.705

plotting $\left(\frac{t_o - t_a}{t - t_a}\right)$ versus time on semi log paper yields; (Figure II-2):

$(\text{Slope})_{\theta=0}$ (extended and read at time 40 sec) = 4.375

$$\frac{mc_p}{A} \quad \frac{0.0857\ lbm \times 0.12\ Btu/lbm\,°F}{0.344\ ft^2} = 2.99 \times 10^{-2}\ Btu/ft^2\,°F$$

$$h = \frac{mc_p}{A} \times \frac{1}{\theta} \ln\left(\frac{t_o - t_a}{t - t_a}\right) = 2.99 \times 10^{-2}\ \frac{Btu}{ft^2\,°F} \times 3600\ \frac{sec}{hr} \times \ln(4.735)$$

$h = 3.97\ Btu/hr\ ft^2\ °F$

From Figure III-3, page II-6; $t_o' - t_a = 2.0°F$

Converting t_o and t_a from millivolts to °F and °R

$t_a = 78.7°F$ $\quad T_a = 538.7\ °R$

$t_o = 122.7 + 2 = 124.7\ °F$ $\quad T_o = 584.7\ °R$

Per Equation [6]:

$$h_r = \epsilon\sigma (T_o^2 + T_a^2)(T_o + T_a)$$

$$h_r = (0.25)(1.714)\left[\left(\frac{584.7}{1000}\right)^2 + \left(\frac{538.7}{1000}\right)^2\right] \times \left[\frac{538.7 + 584.7}{1000}\right]$$

$h_r = 0.304\ Btu/hr\ ft^2\ °F$

$h_c = h - h_r = 3.97 - 0.304 = 3.66\ Btu/hr\ ft^2\ °F$

$$t_{film} = \frac{t_o + t_a}{2} = \frac{124.7 + 78.7}{2} = 101.7\ °F$$

From reference [8], page 359, for $t_{film} = 101.7°F$

$$Y = \frac{\beta g \rho^2}{\mu^2} = 1.75 \times 10^6\ ft^{-3}\ °F^{-1}$$

$k = 1.565 \times 10^{-2}\ Btu/hr\ ft\ °F$

$Pr = 0.72$

For Nu and Gr Pr based on wire diameter:

$d = 2.04 \times 10^{-3}\ ft$; $\quad d^3 = 8.50 \times 10^{-9}\ ft.$

$$(Gr\ Pr)_d = Y \times l^3 \Delta t \times Pr = \frac{1.75 \times 10^6 \times 8.50 \times 10^{-9}\ ft^3 \times 46.0°F \times 0.72}{ft^3\ °F}$$

$(Gr\ Pr)_d = 0.493$ $\quad \log_{10}(Gr\ Pr)_d = -1.693$

$$(Nu)_d = \frac{h_c d}{k} = \frac{3.67\ Btu/hr\ ft^2\ °F \times 2.04 \times 10^{-3}\ ft}{1.565\ Btu/hr\ ft\ °F}$$

$(Nu)_d = 0.479$ $\quad \log_{10}(Nu)_d = -1.680$

For Nu and $G_r P_r$ based on screen diameter

$D = 0.525$ ft $\quad D^3 = 0.145$ ft^3

$$(G_r P_r)_D = \gamma \cdot \ell^3 \Delta t \cdot P_r = \frac{1.75 \times 10^6 \cdot 0.145 \text{ ft}^3 \times 46.0 \text{ °F} \times 0.72}{\text{ft}^3 \cdot \text{°F}}$$

$(G_r P_r)_D = 8.42 \times 10^6 \quad \log_{10}(G_r P_r)_D = 6.926$

$$(Nu)_D = \frac{h_c D}{K} = \frac{3.67 \text{ Btu/hr ft}^2 \text{ °F} \times 0.525 \text{ ft}^3}{1.565 \text{ Btu/hr ft °F}}$$

$(Nu)_D = 123.0 \quad \log_{10}(Nu)_D = 2.090$

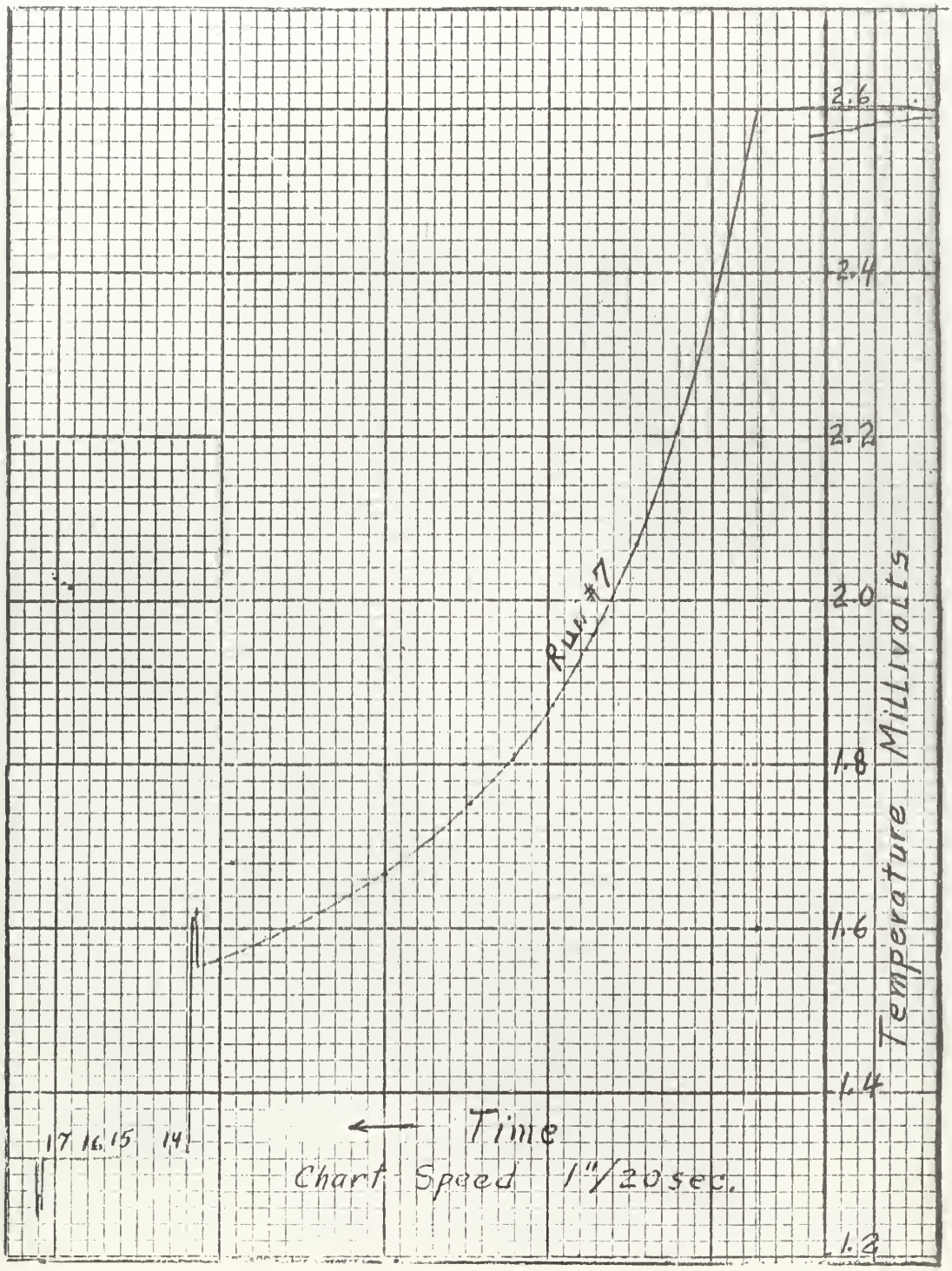

Figure II-1: Recorder chart showing the time-temperature history for run No. 7; 10 X 10 screen.
Temperature Scale: 0.20 mv/in
Time: 20.0 sec/in

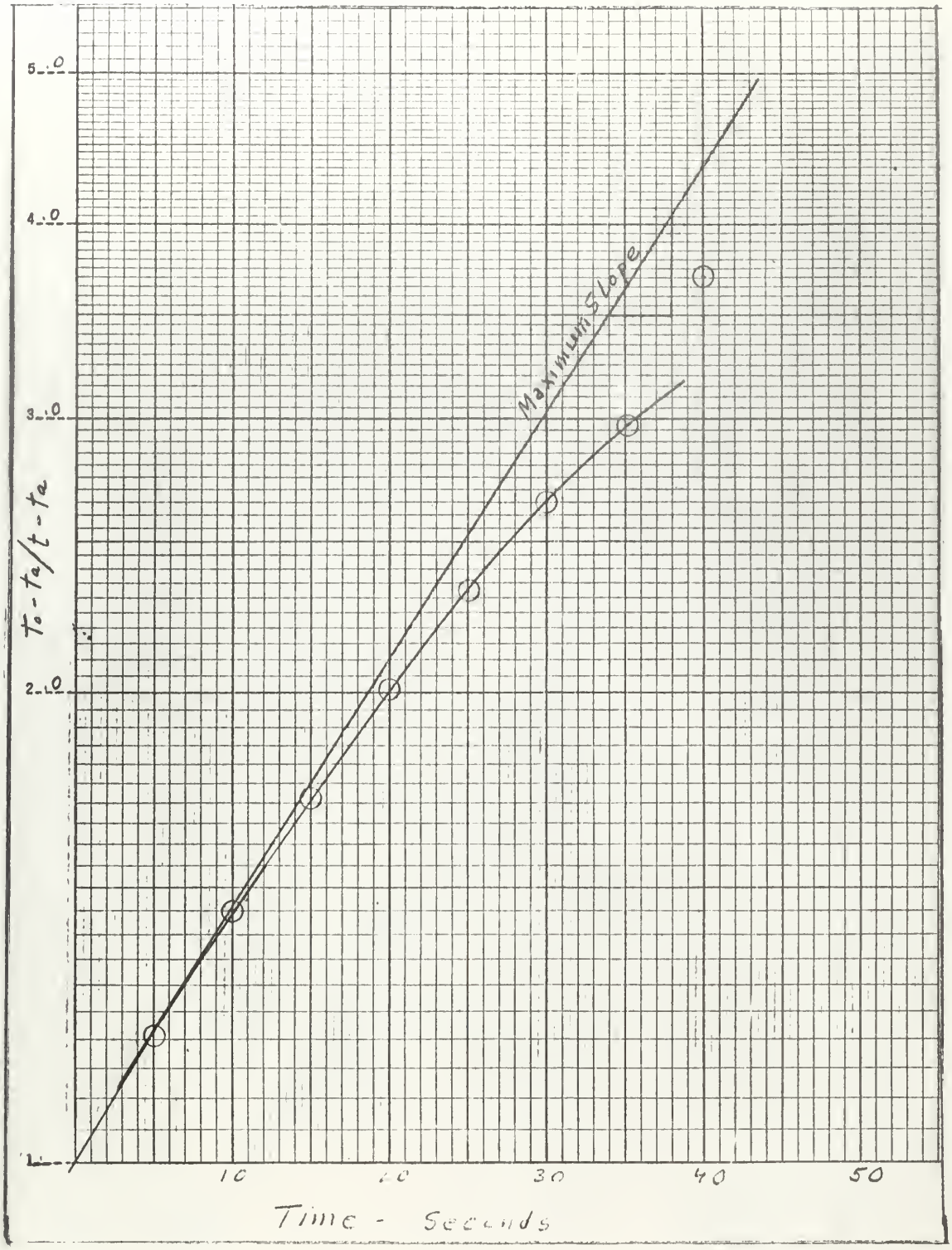

Figure II-2: Semi-log plot of $\ln t_o - t_a / t - t_a$ vs time for run no. 7, 10 X 10 screen. Maximum slope to be used in the calculation of h is shown.

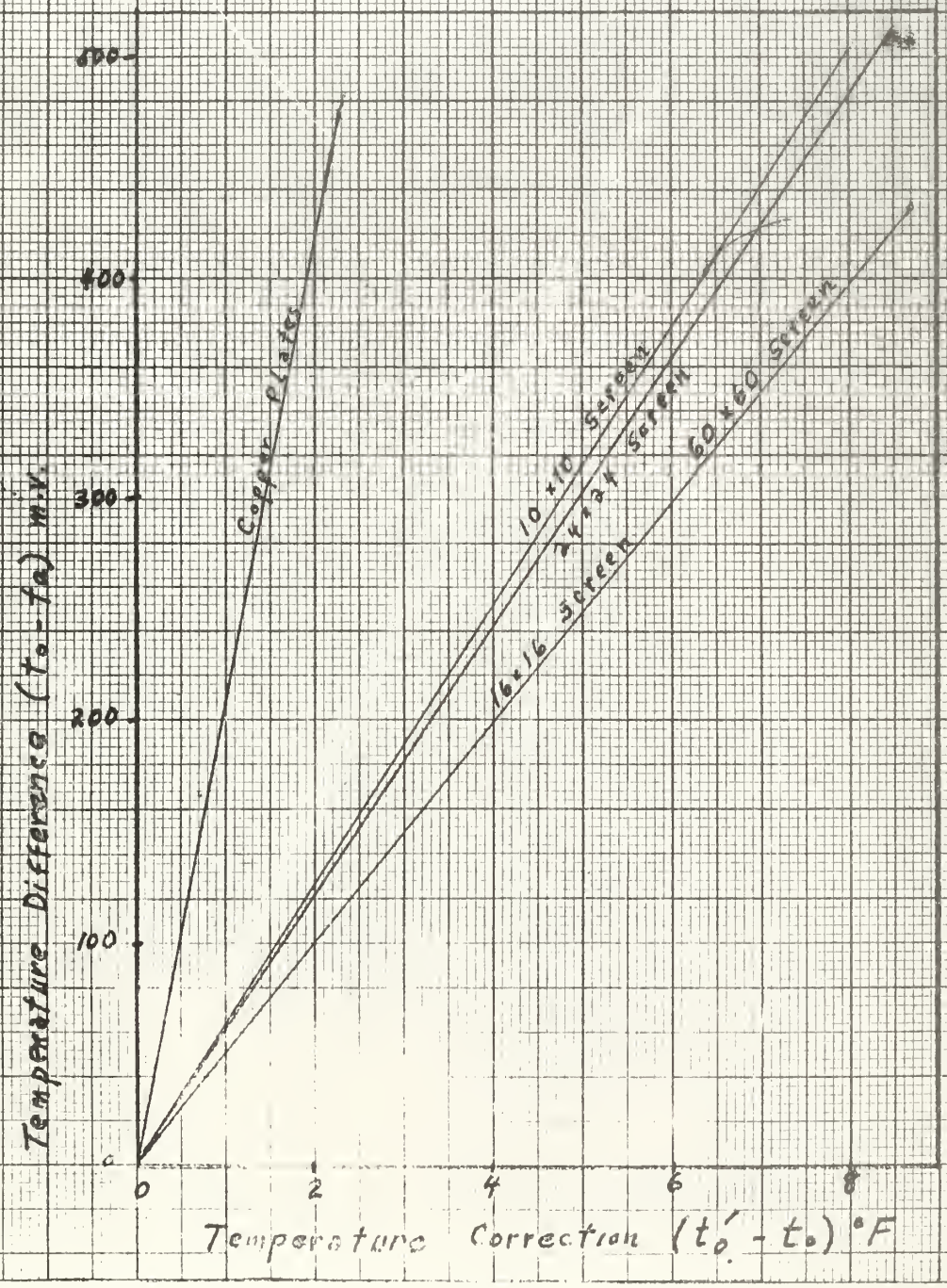

Figure II-3: Thermocouple corrections for 30 gage iron-constantan thermocouples used on test specimens. Results are based on free convection measurements at steady state conditions using a cold body of known temperature, ice, 32 °F, to provide a negative temperature potential with the ambient.